EXPRESSION STUDIES OF THE PROTEOLYTIC p10 FRAGMENT OF THE NEURONAL CDK5 ACTIVATOR IN MAMMALIAN CELLS

CHEN YILIANG

(B.Sc. Fudan University)

A THESIS SUBMITTED

FOR THE DEGREE OF MASTER OF SCIENCE

DEPARTMENT OF BIOCHEMISTRY

NATIONAL UNIVERSITY OF SINGAPORE

2004

Acknowledgements

First of all, I'd like to pay my acknowledgement to my main supervisor, Dr. Steve Cheung for his great support and kind help throughout my research work. He is the one who led me into this research field and inspired me on my research. He is the one who gave me encouragement when I encountered problems in my work. He is the one who has taught me how to deal with and solve all kinds of problems during research. And most of all, he is the one who has taught me patiently on how to be a good researcher. So I cannot even find a word to fully express my thankful feeling to my main supervisor.

Then I want to thank my co-supervisor, Dr. Alan Lee. He has provided not only most of the materials but also good instructions on my bacteria work. And I greatly thank Dr. Robert Qi for providing me all the plasmids I have used in my project.

Next I'd like to thank my labmates: Meng Shyan, Vivien, Yann Wan, Elaine, Shiyi, and Paul. It is my pleasure to work with all of them and I have really got a lot of help from them. And I thank all the people who have given me help during my research.

Finally, I want to pay my special acknowledgement to my parents and my elder brother. Without your love and support throughout my life, I would have done nothing.

Table of Contents

Summary

The protein p10 is a truncated form of $p35^{nck5a}$, a Cdk5 activator. The cleavage of p35 to p25 and p10 under neurotoxic conditions is thought to possibly contribute to neuronal apoptosis in Alzheimer's disease. The work included in this thesis focused on the role of p10 in apoptosis. First, plasmids with p10 cDNA were amplified in bacteria system. Then, the plasmids were delivered into different mammalian cells including Cos-7, HEK293, PC12 and Neuro-2a and p10 fusion proteins were overexpressed in these cells. The influences of p10 overexpression in these mammalian cells were subsequently monitored and studied using a number of biotechniques such as fluorescence microscope, western-blot, immunohistochemistry, flowcytometry and so on. As a result, it was found that overexpression of p10 induced significant cell injury and DNA fragmentation in different mammalian cells. The outcome of this research may lead to an improved understanding of the mechanism of neuronal death in Alzheimer's disease.

List of Tables

List of Figures

Abbreviations

AD: **Alzheimer's disease**

AIDS: **Acquired Immunodeficiency Syndrome**

APOE: **Apolipoprotein E**

APP: **Amyloid Precursor Protein**

ATCC: **American Type Culture Collection**

Aβ: **β-amyloid**

CDC: **cell division cycle**

Cdk5:   **cyclin-dependent kinase 5**

DMEM: **Dulbecco's Modified Eagle Medium**

DMSO: **Dimethyl sulfoxide**

EGFP: **enhanced green fluorescence protein**

EGR: **early growth response**

ERK: **extracellular-signal regulated kinase**

FACS:	**fluorescence-activated cell sorter**
GSK3β:	**glycogen synthase kinase 3β**
KPI:	**Kunitz-type of serine protease inhibitors**
MT:	**microtubule**
Nck5a:	**neuronal Cdk5 activator**
NFTs:	**neurofibrillary tangles**
NGF:	**nerve growth factor**
NPs:	**neuritic plaques**
PCD:	**programmed cell death**
PHFs:	**paired helical filaments**
PI:	**propidium iodide**
PS:	**Penicillin and Streptomycin**
RT:	**room temperature**
TPK:	**tau protein kinase**

CHAPTER ONE:

GENERAL INTRODUCTION

1.1 General introduction of Alzheimer's disease

Alzheimer's disease (AD) is a progressive, neurodegenerative disease characterized by loss of function and death of nerve cells in several areas of the brain leading to loss of cognitive function such as memory and language (Whitehouse *et al.*, 2000). It is the most common cause of dementia although it can be the result of a variety of other processes such as Parkinson's disease, AIDS, head trauma, and alcohol dependence. Patients of AD typically show cognitive impairments leading to characteristic self-care deficits at the end-stage of which they may be unable to walk, to chew or swallow food. Moreover, the cognitive deterioration is often accompanied by mood deterioration as patients may develop depression, anxiety, or delusions (Whitehouse *et al.*, 2000). AD ranks fourth in the cause of death among adults. It will slowly rob its victims of liveliness, savings and dignity. As suggested by epidemiological studies, "up to 4 million people in the United States have AD or a related dementia" (Blechman and Brownnell, 1998). Experts estimate that 22 million people around the world will be afflicted with the disease by 2025. Yet, until now there is no effective way to cure the disease.

1.2 Brief research history of AD

AD was first recognized in 1907 by Alois Alzheimer, a German physician, in his publication, "*A Characteristic Disease of the Cerebral Cortex*" (Alzheimer 1907). In his paper, he described "a 51-year-old woman from Frankfurt who had exhibited progressive cognitive impairment, focal symptoms, hallucinations, delusions, and psychosocial incompetence" (Whitehouse *et al.*, 2000). From then on, the scientific concept of AD has undergone a continuous advancement as skills and technologies of scientific research improve. AD was first characterized by clinicians as a pattern of progressive cognitive impairment. It was originally used to describe presenile dementia and later extended to the dementia among the elderly. The second important step of the concept of AD was the clear characterization of the disease state. The term *dementia*, which predates AD, means an organic mental disorder characterized by a general loss of intellectual abilities involving impairment of memory, judgment and abstract thinking as well as changes in personality. It was differentiated from mental retardation because dementia requires normal intellect which is impaired after the onset of the disease. Dementia was also differentiated from *delirium*, which was characterized by reduced ability to maintain attention to external stimuli and disorganized thinking as manifested by rambling, irrelevant or incoherent speech. Then the development of the techniques to examine brain tissues made it possible to develop theories about etiology and corresponding therapeutic strategies. As an example, the effective silver staining techniques are crucial to the discovery of neurofibrillary tangles which are the hallmark

of AD. Later electron microscopy showed more details of the plaques and tangles not possible with a microscopy to the researchers. Meanwhile, the advancement of neurochemistry especially about characterization of neurotransmitters threw new light on the AD research. The success in Parkinson disease was modeled by AD researchers. In Parkinson disease, the neurotransmitter dopamine was considered related to the cell loss in the substantia nigra. The compounds capable of increasing the dopamine level were discovered to effectively reduce the clinicopathologic symptoms. In AD, the loss of chemical markers for the neurotransmitter acetylcholine was found. So the application of increasing the acetylcholine level was developed several years later and brought some benefits for AD patients. Thus AD as a clinical entity changed into a neurochemical entity. Now with the emergence and advancement of molecular biology, AD is regarded as a genetic disease. Early onset AD patients were found to have at lease one other family member with the disease. Strong genetic mutations on some genes cause a predisposition to AD. For instance, researchers discovered that plaques and tangles appeared in the brains of Down syndrome patients when they lived beyond the age of 40. Many also developed a dementia. As Down syndrome is caused by an extra copy of 21st chromosome, researchers managed to find mutations in this chromosome causing AD in certain families (Head and Lott, 2004). As another example, the gene for apolipoprotein E (APOE) which locates on the 19th chromosome is also considered to link to AD (Harwood *et al.*, 2002). People with homozygote for the APOE-4 allele are more at risk for AD while those with APOE-2 less so.

In summary, the characterization of AD develops from the anatomic/pathologic level to the neurochemical/neurotransmitter level and now to the molecular/genetic level. Since the recognition of AD, what we think of it has changed tremendously. Although we have already improved the diagnosis and treatment of AD, it remains to be discovered how biological and social factors interact to cause AD which may lead researchers to find methods to effectively cure and even prevent AD.

1.3 Psychopathological Symptoms and Syndromes of AD patients

Major depression is "a syndrome characterized by a sustained dysphoric mood, a change in self-attitude toward worthlessness, feelings of helplessness or guilt, and a general pessimism" (Terry *et al.*,1994). These moods are often accompanied by loss of interest in activities in the absence of external precipitants and change in eating habits, insomnia, early morning wakening, decreased sexual drive, fatigue and suicidal thoughts. It was reported that the major depression syndrome occurs in 15% to 20% of AD patients. The depressive syndrome often occurs early during the progress of the disease, most often within the first 3 years. Depressed AD patients are more likely to be institutionalized than nondepressed ones and have higher mortality rates.

Anxiety, *irritability*, and *restless overactivity* emerge at a later stage of AD. Sometimes the syndrome appears alone and sometimes secondary to major depression, delusions, or hallucinations. For example, some patients have the anxious, irritable syndrome as a result of their concern of having lost something. So they wander about and aimlessly

search through drawers and closets. Some patients rise anxiety for fear of losing track of their caregivers. So they may persistently follow their caregivers around the house.

Delusion is another common psychopathological symptom among AD patients. Delusions are "false ideas that are impervious to persuasion, are idiosyncratic and preoccupying, and affect the person's behavior" (Terry *et al.*,1994). It was reported that 40% of AD patients experienced delusions during the illness. The most common delusion they experience is that somebody is stealing things from them. There are other delusion examples. In one example, a patient insisted that he was 10 years younger than birth record indicated and repeatedly tried to contact the appropriate authorities to correct it. Some patients thought that their spouses were their mothers or their children their siblings, or they even failed to recognize their family members. Some patients claimed that the house they were living in was actually not their home and that they must return home, or that there were other people living in the house. In AD, delusions normally occur during early to middle stage of the illness which is 2 to 4 years after onset on average. Sometimes AD patients show aggressive behavior when caregivers try to stop them from acting on the delusions.

Hallucinations are false perceptions occurring without any true sensory stimulus. The patients may see, hear, smell or feel things that are not present. Hallucinations in AD are generally signs of rapid decline of recognition and rapid deterioration of the disease. In addition to abnormal moods, beliefs, and perceptions, abnormal behaviors can be directly observed from AD patients. Deterioration of many *learned behaviors* occurs about 2 to 3 years after the onset of the syndrome. This phenomenon is believed to be

associated with the spread of neuropathological changes to the parietal lobes. These learned behaviors include socially appropriate behaviors such as the ability to speak, write, calculate, dress, bathe, and toilet which will be gradually lost during the progress of AD. Moreover, some complex behaviors such as driving an automobile, making a plan, and cooking meals deteriorate early in the disease course. All of the above behavior impairments can be described as aphasia and apraxia (Terry *et al.,*1994).

Aggression was reported in 20% to 57% of the cases. The majority of the cases were directed toward other people or objects. The aggressive behaviors can be caused by environmental antecedents, as when a patient is confined against his/her will. The aggression behaviors are often accompanied by various behaviors such as crying, cursing or hitting.

Many AD patients have *repetitive behaviors* which mean they continuously repeat some actions without satisfying themselves or concluding the actions. For example, some patients start to walk and refuse to rest. They just want to walk but have no idea where they are walking to. Some patients clap their hands on and on, others fold and refold laundry over and over. They may perform these actions continually for hours. Although they seem to have a purpose in mind to do so, they cannot articulate what the purpose is (Terry *et al.,*1994).

Finally, AD patients display many other behaviors which are not yet well defined. For example, *agitation* is used for various behaviors that have different antecedents. Similarly, the word *wandering* describes behaviors with various forms and arises from different situations. The patients may wander because they have the delusion of having

lost something and search for it, or because they are driven by a vague purpose in mind mentioned in repetitive behaviors above.

All the psychopathological symptoms are thought to be associated with the course of AD as AD is an abnormal condition spread through the brain. Although researchers managed to describe the pattern of cognitive symptoms at different stage of AD, the relationship between the pattern of noncognitive symptoms and the course of the disease remains to be elucidated.

1.4 Molecules implicated in the pathogenesis of Alzheimer's disease

There are two hallmarks of AD: neurofibrillary tangles (NFTs) and neuritic plaques (NPs). So far, the relationship between the NFTs and NPs is still unclear and under intensive investigations although much information has been extracted from both of them.

NFTs are a compact filamentous network occupying the whole of the cytoplasm in certain classes of cell in the neocortex, hippocampus, brainstem, and diencephalons. The number of the tangles, as seen in postmortem histology, correlates with the degree of dementia during life. NFTs are formed by paired helical filaments (PHFs). And the major component of PHFs is hyperphosphorylated tau protein, a microtubule-associated protein (Ihara *et al.*, 1986). In normal conditions, this protein takes part in the assembly of microtubules, the stabilization of microtubules, and connecting them with other cytoskeletal filaments. The equilibrium between phosphorylations and dephosphorylations of tau modules is important for maintaining normal function of

cytoskeleton and consequently axonal morphology. Hyperphosphorylation of tau is believed to initiate the pathological process. Following that, cross-linkages among tau proteins occur and insoluble fibrils that cannot be degraded by parent cell form. Then they begin to accumulate and crowd in the cell body.
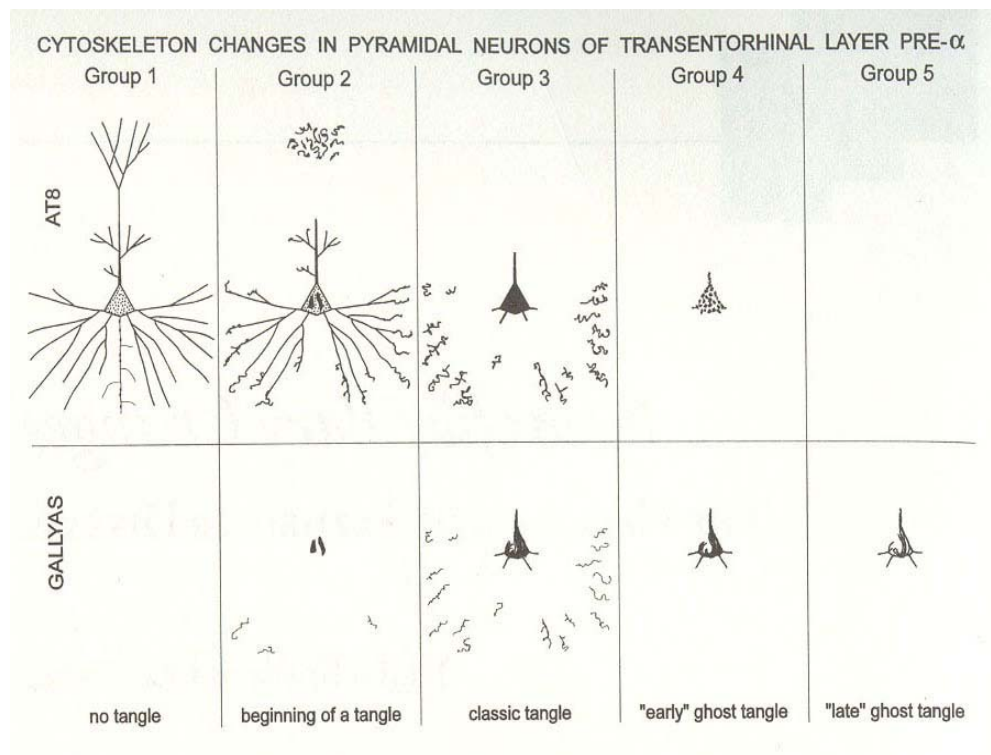
Figure 1.1 Schematic drawing summarizing immunostaining of the phosphorylation-dependent anti-tau antibody AT8, compared with the corresponding Gallyas silver staining of developing neurofibrillary tangles. The progression of pathological changes of the neuronal cytoskeleton is shown from the group 1 to group 5 (Whitehouse *et al.*, 2000).

The newly developed antibody, AT8 that binds to phosphorylated tau protein provides a way to observe the process of the cytoskeletal changes (Figure 1.1). Firstly, the tau protein is still soluble and nonargyrophilic. It fills the perikaryon and dendrites and

axon. In this pretangle stage, NFTs composed of abnormal phosphorylated tau protein have not appeared. The nerve cell maintains its normal shape. This kind of cells first appears at certain site of AD-related lesions with initial changes in the cytoskeleton in the absence of beta-amyloid deposits and other obvious pathological lesions. Later, cross-linked and argyrophilic precipitates start to occur. The distal segments of the dendrites turn to twisted and dilated and probably detach from the proximal stem. Meanwhile, NFTs appear in the cell body. In the final stage of the deterioration, after years of development in the cells the NFTs gradually become less and less densely twisted and lose much of their argyrophilia until completely disappeared.

As mentioned above, tau protein is an essential element of PHFs. The phosphorylation and dephosphorylation status of tau appear to influence the protein's structure and conformation which determine its binding ability to tubulins and the capacity to assembly microtubules. The tau protein has different phosphorylated sites in PHFs from Alzheimer brains (Figure 1.2).
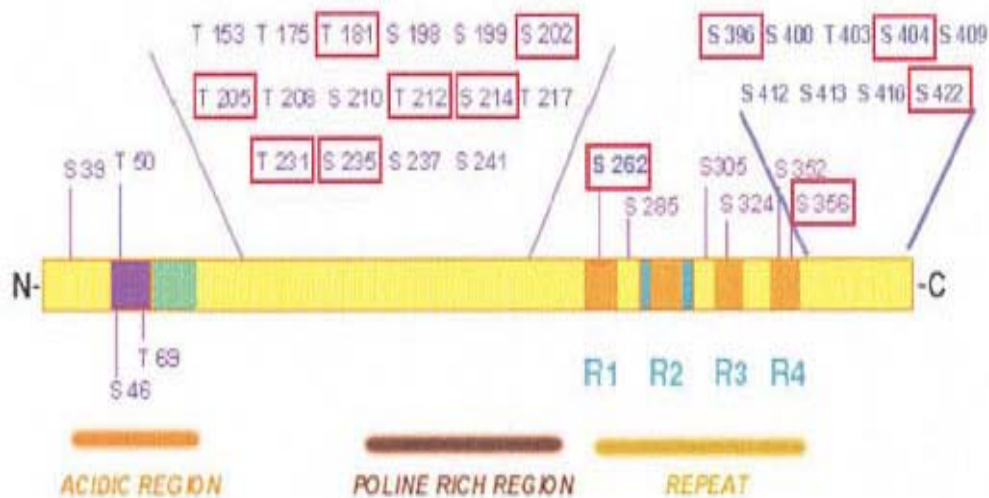
Figure 1.2 Schematic representations of the tau protein domains and its phosphorylation sites, indicating the hyperphosphorylated sites (rectangles in red) found in paired helical filaments in AD. Tau hyperphosphorylations block its capacity to modulate cytoskeletal dynamics and promote tau self-aggregation into PHFs and tangles. The microtubule binding repeats are denoted by R1 through R4 (Maccioni *et al.*, 2001).

Two tau protein kinases, TPK I and TPK II, were found to be the most two possible kinases responsible for the tau hyperphosphorylation in the formation of PHFs (Ishiguro *et al.*, 1992; Arioka *et al.*, 1993). Most of the 10 major phosphorylation sites of tau in PHFs are phosphorylated by the two TPKs. TPK I was also called glycogen synthase kinase 3β (GSK3β) while TPK II consists of two subunits, an activator subunit p35 and a catalytic subunit cyclin-dependent kinase 5 (Cdk5). TPK I can phosphorylate those tau proteins that are already phosphorylated to certain extent, but it can not phosphorylate completely dephosphorylated tau. In contrast, TPK II can phosphorylate

both. The phosphorylation of tau by TPK I can induce an apparent molecular weight

shift and the formation of the PHF epitope while TPK II cannot. But prior

phosphorylation of tau by TPK II may enhance TPK I phosphorylation. So it is believed

that the two TPKs cooperate in both normal functions and pathological processes

(Imahori *et al.*, 1997).

Another hallmark of AD, neuritic plaques are formed mainly by a 4-KDa peptide with a

significant beta structure called beta-amyloid (Aβ). The Aβ peptide is derived from the

amyloid precursor protein (APP) by proteolytic cleavages (Figure 1.3).
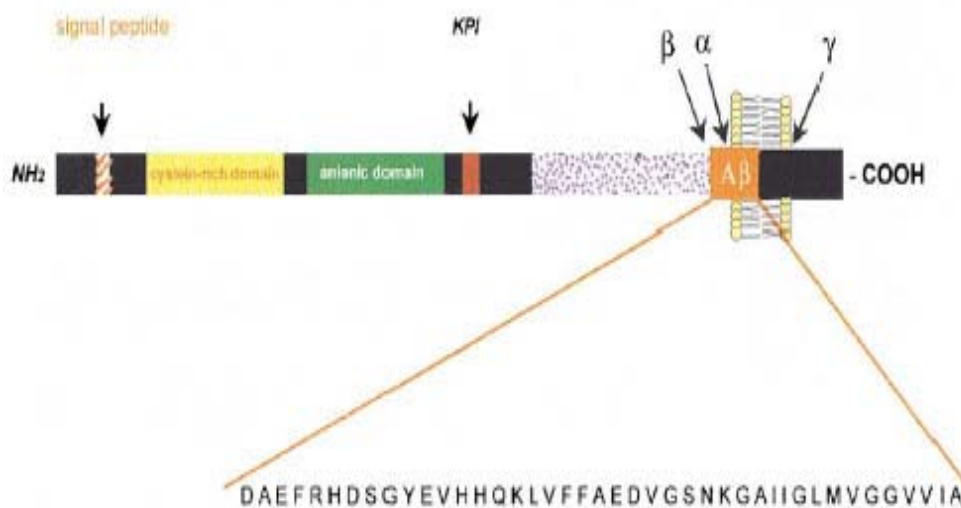
Figure 1.3 Schematic representation of the amyloid precursor protein major domains,

indicating the sequence of the 4-KDa Aβ peptide (in orange) cleaved by secretases

(Maccioni *et al.*, 2001).

APP is a single transmembrane polypeptide with its N-terminal facing extra cellular

space and C-terminal inside cytosol (Kang *et al.*, 1987). It is highly conserved during

evolution and expressed by all mammals already sought. Moreover, it is not a neuron

specific protein as many other brain cells and peripheral cells also express APP. It comprises a heterogeneous group of polypeptides which are caused by alternative splicing process. The largest splicing form contains 770 amino acids as shown in Figure 1.3. It has a signal peptide near N-terminal for translocation and a motif homologous to the Kunitz-type of serine protease inhibitors (KPI) (Kitaguchi *et al.*, 1988). The transmembrane domain is near the C-terminal. It is posttranslationally modified through the secretory pathway during and after which it undergoes a variety of proteolytic cleavages by secretases. Then the cleaved APP products of the secretases can be secreted into the extra cellular space or kept in cytosol. The cleavage sites of α-secretase and β-secretase are just on the N-terminal side of transmembrane domain while that of γ-secretase is interestingly in the middle of transmembrane domain. Normally APP is cleaved by α, γ-secretase or alternatively by β, γ-secretase. Aβ is one of the products of β, γ-secretase (Maccioni *et al.*, 2001).

Normally there are two Aβ variants: Aβ (1-40) and Aβ (1-42) because γ-secretase cuts APP at residue 711 or 713. However, Aβ (1-42) has a much higher capacity to self-aggregate and forms amyloid plaques (Pike *et al.*, 1995). Although Aβ generation was previously assumed to be a pathological event, recent researches reveal that Aβ production is a normal metabolic process. Actually, it can be detected in cerebrospinal fluid and plasma of healthy cells throughout life. The normal functions of APP and its cleaved products remain to be further discovered. But a number of possible functions have been attributed. For example, the isoforms that contain the KPI domain may play a role in the inhibition of prohormone thiol protease (Hook et al., 1999). They may also

have the function of cellular adhesion and neuroprotection. Moreover, several recent studies suggest that APP may be a membrane cargo receptor for Kinesin-I and might help to connect Kinesin-I with certain subset of axonal transport vesicles (Maccioni *et al.*, 2001).

The gene for APP is on chromosome 21. Mutations within the sequence coding for Aβ cause higher Aβ production or increasing of its ability to self-aggregate which consequently generates amyloid plaques. The anomalous amyloid deposition was shown to clearly associate with the pathogenesis of AD.

1.5 Cdk5/p35 pathway and Alzheimer's disease

Cdk5 is a serine/threonine kinase and belongs to the cyclin-dependent kinase (Cdk) family (Lew *et al.*, 1995). It was first identified around 1991 and purified from bovine brain in 1995 since which it has been under intensive research on its potential role in diseases. Although Cdk5 is expressed in many tissues, its activity is detected nearly only in brain extracts. Moreover, Cdk5 shows a phosphorylation site specificity similar or identical to the cell cycle regulatory kinase, cdc2 kinase. So it was originally named as neuronal Cdc2-like protein kinase. Cdk5 displays 60% homology to Cdk1 (Fang and Newport, 1991; Meyerson *et al.*, 1991). Similar to other Cdks, monomeric Cdk5 shows no enzymatic activity but unlike other Cdks, it is not regulated by cyclins. Its activation requires association with either of the two brain specific regulatory proteins called p35

and p39 which have little sequence similarity to cyclins although p35 assumes a cyclin-like fold suggested by structural studies (Tsai *et al.*, 1994; Tang *et al.*, 1995).

The normal roles for Cdk5 in the brain already known associate with neuronal migration, axon growth and synaptic function (Smith *et al.*, 2001).

Neuronal migration: some studies dealing with the homozygous deletions in the p35 and Cdk5 genes showed that Cdk5 is likely to be involved in neuronal migration (Chae *et al.*, 1997; Ohshima *et al.*, 1996). In the normal cortex, neurons are organized into six different layers. Newly differentiated postmitotic neurons migrate through certain routes to form the six layers. One of the well-studied routes is displayed by neurons derived from epithelium in the cortical ventricular zone (Parnavelas *et al.*, 2000). These cells migrate via the process of radial glia and take the positions in the cortex in an "inside-out" form. That is, newly formed neurons in the outermost layers migrate through previously formed layers and form the inner layers. However, the "inside-out" layer form is inverted in p35$^{-/-}$ mice. The migration of newly formed neurons is disturbed and they tend to pile up under previously formed neurons. Although p35$^{-/-}$ mice are quite vulnerable to early lethality, they can be fertile and live up to adulthood. But Cdk5$^{-/-}$ mice die in embryogenesis or at birth which suggests that p35 alone is not capable of maintaining all Cdk5-dependent functions. The migration defect among cerebella neurons without Cdk5 was proved to be cell autonomous which may be evidence that Cdk5 plays a role in the migrating cells (Ohshima *et al.*, 1999). That mice with mutations in p39 show no obvious abnormalities suggests p35 may substitute p39 to some extent. Nevertheless, mice with mutations in both p35 and p39 die before birth

showing the same brain abnormalities as in Cdk5$^{-/-}$ mice (Elledge *et al.*, 1991). This indicates that p35 and p39 together are necessary and enough to play Cdk5 regulating role in neuronal migration. Whether p35 and p39 bear different substrate specificities remains to be studied, but cell fractionation experiments discover that they may appear in different subcellular sites (Humbert *et al.* 2000a&b).

Axon growth and extracellular signals: p35 and Cdk5 knockout mice show defects in fasciculation in some axon tracts (Kwon *et al.*, 1999). Several relevant experiment results also point to the possibility of Cdk5's direct role in axon growth. Firstly, both Cdk5 and p35 are in axon growth cones (Nikolic *et al.*, 1999). Secondly, neurons with Cdk5 activity inhibited display reduced ability to grow axons. Thirdly, disrupting Cdk5 function results in errors in axonogenesis. In addition to axon growth, Cdk5 activity is also shown to involve in many extracellular signal pathways such as cadherin pathways and non-receptor tyrosine kinases pathways. Moreover, studies on Cdk5 interactions and its substrates are uncovering the roles of Cdk5 in terms of cytoskeleton systems.

Synaptic functions: p35 knockout mice have lowered threshold for lethal seizures. And Cdk5, p35, and p39 are present in synaptic membranes subcellular fractions. What is more, immunogold labeling experiment shows that p39 localizes to pre- and postsynaptic compartments (Humbert *et al.* 2000b). All of the above point to the potential role these kinases may play in synaptic function. Consistently, Cdk5 is also found to function at synapses.

As Cdk5 activity is involved in so many cell processes, it is natural to assume that Cdk5 activity is tightly regulated in neurons. Actually, several papers have indicated that the

Cdk5 regulatory protein, p35, may be highly regulated by its subcellular localization and stability (Patrick *et al.*, 1999;Lee *et al.*, 2000). Deregulation of Cdk5 activity especially the hyperactivity of Cdk5 is proved to be toxic to neurons and may contribute to such neurodegenerative disease as Alzheimer's disease.

Among so many Cdk5 substrates, just a few of them turn out to be the candidates responsible for AD. One is β-catenin as it interacts with presenilin-1 protein. Mutations of the presenilin-1 gene are the main reason of familial, early-onset AD. Mutant presenilin-1 shows reduced ability to interact with and stabilize β-catenin, causing it to be increasingly degraded (Zhang *et al.*, 1998). Interestingly, AD patients with mutant presenilin-1 also display reduced β-catenin levels. As phosphorylation of β-catenin by p35/Cdk5 influence the association of presenilin-1 and β-catenin (Kesavapany *et al.*, 2001). The deregulation of this pathway may associate with the cause of AD. Another major candidate is tau, a microtubule-associate protein. Neurotoxic molecule β-amyloid (Aβ) induces cleavage of p35 to two subunits, p25 and p10 which is mediated by a calcium-dependent cysteine protease called calpain (Lee *et al.*, 2000). Association of p25 and Cdk5 forms the Cdk5/p25 complex which displays higher ability than Cdk5/p35 complex to phosphorylate protein tau. Since hyperphosphorylated tau is well known to be the major component of paired helical filaments (PHFs) which form neurofibrillary tangles (NFTs), one of the two hallmarks of Alzheimer's disease, Cdk5/p35 regulation pathway becomes one of the hottest research topics on Alzheimer's disease. The tau protein is capable of inducing microtubule (MT) assembly under normal conditions. It is surmised that hyperphosphorylation of tau may interrupt

its MT assembly ability and thus disrupt cytoskeleton leading to neuron degeneration. Actually, several groups have reported that tau is essential to Aβ induced neurotoxicity process which involves increase of the Cdk5 activity while MT-stabilizing reagent like taxol decreases Aβ toxicity (Rapoport *et al.*, 2002; Li *et al.*, 2003). What's more, morphological analysis suggests that neurons with mouse or human tau expressed degenerate in the presence of Aβ while tau-depleted neurons display no signs of degeneration in the presence of Aβ. All the above evidences point to the important role tau protein has played in the Aβ-induced neurotoxicity leading to neurodegeneration in the central nervous system. (Fig. 1.4)

As p35 and p39 are the only known Cdk5 activator so far and their expression level is the main determinant of the Cdk5 activity, it is necessary to explore the metabolism of p35 and p39. As mentioned previously, p35 and p39 are almost exclusively expressed in differentiated neuronal cells. When neuronal cells PC12 are differentiated by nerve growth factor, the expression of p35 can be quickly induced and enhanced by extracellular stimuli such as neurotrophic factors, especially those acting via the ERK/Egr pathway (Harada *et al.*, 2001). However, p35 is a short-lived protein in vivo and its degradation determines the life span. It was reported that the phosphorylation of p35 by Cdk5 served as a signal for ubiquitination and degradation by proteasomes (Patrick *et al.*, 1998). Thus, the phosphorylation of p35 by Cdk5 plays an autoregulatory role on Cdk5 activity. Under certain conditions, calpain is activated and cleaves p35 to p25 and p10 which is thought to be probably implicated in the cytotoxicity in AD brains. On the other hand, the expression of p39 is similar to p35 in

adult brains. Moreover, the proteolytic pathway and cleavage of p39 is also similar to that of p35. The cleaved products of p39 are p29 and p10 but it is not known whether they are detected in pathological neurodegenerative neurons.

Why is p25 more toxic than p35? What is the mechanism that p25 leads to neurodegeneration? One group proposes that since p35 contains an N-terminal myristoylation signal motif that anchors p35 to cell membranes (Liu *et al.*, 2003), p35 may be confined to certain part of the neurons and under spatial regulation (Patrick *et al.*, 1999). p25 is the C-terminal part of p35. Abnormal conversion of p35 to p25 may increase p25 level and dislocate p25 causing Cdk5 sequestered from normal regulation system and concentrated at abnormal sites. Thus, Cdk5 may phosphorylate substrates not normally phosphorylated by it or hyperphosphorylate its substrate such as tau protein. It is also reported that p25 is more stable than p35. So the increased ratio of p25/p35 may somewhat contribute to the abnormal increased Cdk5 activity in the AD patients' brains both by mislocalization of p25 and by prolonged existence of p25. (Fig. 1.4)
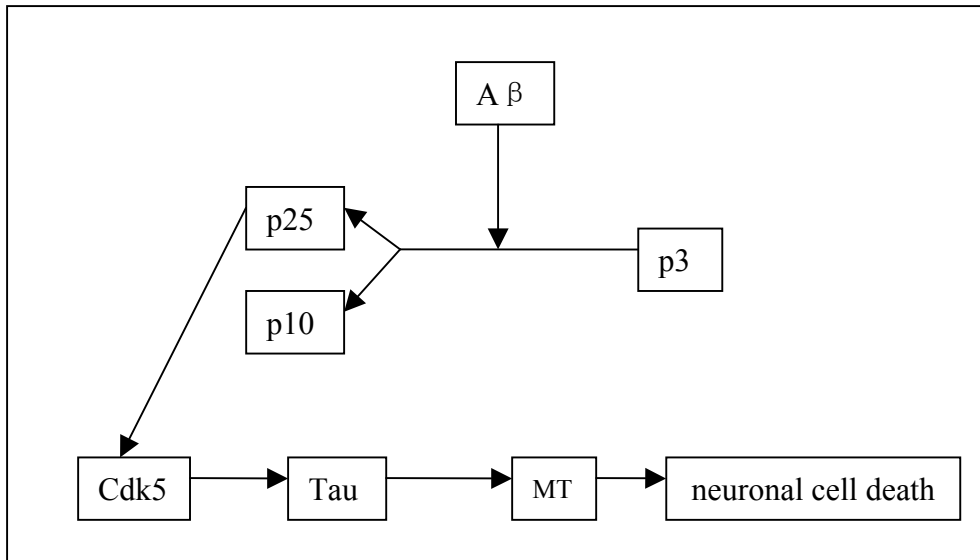
Fig. 1.4 The possible deregulation of Cdk5/p35 pathway: the cleavage of p35 to p25 induced by Aβ toxicity is followed by the formation of Cdk5/p25 complex which hyperphosphorylates tau proteins because of dislocation of p25 and prolonged existence of p25. Hyperphosphorylated tau proteins tend to self-aggregate and reduce the ability to assembly microtubules that consequently causes disruption of cytoskeleton leading to neuronal cell death.

However, the theory of p25 in AD brains encounters many problems. For example, opposing results have been reported in terms of whether conversion of p35 to p25 causes hyperphosphorylation of tau protein. One group has shown that overexpression of Cdk5/p25 complex in cos-7 cells gives higher tau phosphorylation than that of Cdk5/p35 complex (Patrick *et al.*, 1999). But another group has proved that the cleavage of p35 to p25 in rat neuronal cells is accompanied by increased activity of Cdk5 but not by tau hyperphosphorylation (Kerokoski *et al.*, 2002). On the contrary, tau phosphorylation decreases at multiple sites. Inhibition of calpain in neuronal cells

treated by glutamate toxicity has no obvious effect on tau phosphorylation which implies that calpain-mediated processes including cleavage of p35 to p25 do not contribute to tau phosphorylation. Moreover, Takashima and his colleagues have reported that overexpression of p25 in rat neuronal cells does not show altered phosphorylation of tau proteins (Takashima *et al.*, 2001). In another example, there are conflicting results on p25 levels in AD brains. On one hand, Tsai and her colleagues reported that compared to control brains p25 level accumulated by 20-40-fold in seven out of eight AD brains (Patrick *et al.*, 1999). This group also showed later that mean p25/p35 ratios were about 1.7 and 5 for control and AD brains respectively (Tseng *et al.*, 2002). One the other hand, Tandon and his colleagues pointed out that no elevation of p25 levels was found in the 22 AD brains tested (Tandon *et al.*, 2003). On the contrary, p25 immunoreactivity appeared lower in AD brains. Their results are compatible with other ones showing that there is no difference in p25/p35 ratios between control and AD brains (Takashima *et al.*, 2001; Taniguchi *et al.*, 2001; Yoo *et al.*, 2001). So the mechanism that underlies AD brain may be more complicated. But I notice that among the literature of the Cdk5/p35 pathway, when talking about the cleavage of p35, almost all attention was drawn to p25, the C-terminal cleavage fragment of p35. Another cleavage subunit p10 has been long neglected by researchers. As implied in the previous passage, p10 is the N-terminal cleavage fragment of p35. And the N-terminal regions of p35 were reported to be responsible for its binding to other intracellular components such as cell membrane (Dhavan *et al.*, 2001), nuclear proteins (Qu *et al.*, 2002), and possibly Golgi apparatus (Paglini *et al.*, 2001), forming

large complex in vivo. However, whether binding of p35 to the larger complex is the only function of p10 before cleavage is not clear. Moreover, what happens to p10 after cleavage is not known yet.

1.6 Alzheimer's disease and aging

The phenomenon of aging can be defined as the gradual changes in the structure and function of animals that occur with the passage of time, that do not result from disease or other gross accidents, and that eventually lead to the increased probability of death as the animal grows older. It has long interested scientists for obvious reasons. People long to know why higher life forms especially humans inevitably age and die. Are aging and death just unfortunate negative characteristics that natural selection has endowed many life forms by accident or positive strategies of lives for continuous survival as species instead of as individuals? Is it possible to avoid both of them? Unfortunately, all the questions above seem far from being answered. We are still too ignorant to wholly uncover this mystery. However, with endless effort and myriad insightful exploration, scientists have shed more and more light on this topic.

The aging process should be viewed as an extreme complexity that arises from and is influenced by both genetic and environmental factors throughout the life span and probably transgenerationally. It is not the result of a single molecular process. We may take the nervous system as an example. The condition of the nervous system is the result of infinite genetic and environmental events. Throughout a human's life, the

influence of hereditary determinants is subject to various environmental influences such as social environment (e.g., the increased risk of depression and mortality after the death of a spouse) and nutrition (e.g., some research on rodents showed that diet restriction is associated with slowing of aging processes) and so on. Moreover, the impact of the genetic and environmental factors may vary greatly. Some are temporary while others are life-long existing and cumulative. Some are reversible while others are irreversible. So each individual is the product of myriad factors interwoven with a unique pattern.

Despite individual variations in the aging process, there is an overall consistency in the characteristics of aging which is called a canonical pattern of aging. For instance, an age-related loss of germ cells and hormone-producing follicles is the main cause of sterility at midlife. There are many other canonical aging changes of mammals such as the accumulation of aging pigments in nondividing cells, the decrease of striatal dopamine receptors, and the proliferation of smooth muscle cells in blood vessel walls and so on. The identification of the canonical aging changes and further research on why and how they happen may be a promising way to understanding the phenomena of aging. And we may have another way to achieve this goal by the research about age-related diseases such as Alzheimer's disease for such disease provides us a chance to compare normal human tissues with abnormal ones and subsequently find certain factors that may be responsible for the diseases. As the diseases are age-related, thus we find a way to sieve through myriad factors and pick out candidates associating with age and finally to find out which ones are responsible for age.

Now here is an important question: how is Alzheimer's disease related to aging at the molecular level? So far, there is no widely accepted answer but Chen et al., have put forward a promising theory based on comprehensive works of their own and others (Chen *et al.*, 2001). They propose that the hallmarks of AD, plaques and tangles, are "the results of metabolic inefficiency (especially in Ca^{2+} signaling), a natural event in aging." Just like that of cholesterol deposition, aging itself may trigger the formation of plaques and tangles. When the progress is enhanced by risk factors, it can lead to late-onset sporadic Alzheimer's disease. The details of the theory are summarized below:

1. Metabolic inefficiency is a natural event in aging

Aging process is currently thought to be controlled and pushed by a "genetic clock" which is not fully identified yet. But an obvious expression of aging may be the decline of energy metabolisms after about age 30 which consequently slowdown myriad metabolic pathways. The metabolic slowdown then consequently leads to many signs of aging in the body which intensify throughout the following years. With the accumulation of the changes, numerous aging markers appear such as hair graying, bone loss, cholesterol deposit, plaques and tangles.

2. Mechanism of amyloid plaque formation

Plaques and tangles are the most obvious markers in aging and AD brain, according to this theory, their appearance is simply due to inefficient normal processing of APP and

tau respectively. Now let's consider APP first. In vivo, APP is processed by two pathways: normal α-processing during which APP is cleaved by α-secretase, or amyloidogenic processing by β- and γ-secretase (Figure 1.3). The three possible mechanisms for Aβ overproduction during aging are: (i) APP gene overexpression; (ii) overactivation of both β- and γ-secretase; and (iii) inactivation of α-secretase. The first one has been studied and largely ruled out as a common cause of the disease. The second one seems promising. However, it can hardly provide a necessary rationale: why and how can β- and γ-secretase become overactivated during normal aging? As amyloid plaques are apparently a natural event during normal aging, any proposed mechanisms that cannot be ultimately explained by normal aging have to be logically ruled out. Then the most reasonable model for Aβ overproduction is the third scenario: α-secretase inactivation. Because secreted APP (APP_s) is just one of the myriad secretory proteins that are physiologically released for normal function such as cell growth, differentiation or maintenance. When cell growth and other normal processes slowdown during aging, naturally so will the secretion of APP_s. The reduction of APP_s secretion in turn causes the accumulation of the APP which prone to be increasingly attacked by other proteases such as β- and γ-secretase. Thus, Aβ overproduction appears during aging and because of aging.

3. Mechanism of tangle formation

According to this theory, the inefficient normal degradation of tau is responsible for tangle formation. Cytoskeleton is a dynamic system within the cells as the temporary

break-up and reconstitution of the cytoskeleton is required during cell growth, division and differentiation. Proteolytic degradation is known to be involved as an essential step in this process. Obviously, direct proteolysis of the major cytoskeleton proteins such as actins and tubulins is too disruptive. Instead, proteolysis is normally operated on the cytoskeleton cross-linking proteins such as filamin, fodrin or tau. In addition, these proteins also undergo a dynamic phosphorylation-dephosphorylation process which may change their vulnerability to protease degradation. In this model, tau undergoes a regulatory process in response to Ca^{2+} signals in neurons through life. But during aging, basic metabolisms including Ca^{2+} signaling may decline which consequently inactive many Ca^{2+}-dependent enzymes. Some of those enzymes may be responsible for the phosphorylation status of tau or even degradation of it. Thus, the reason of tau hyperphosphorylation and accumulation in aging brains is traced back to aging itself.

1.7 Programmed cell death in Alzheimer's disease

Programmed cell death (PCD) is activated by an indigenous cell signaling system leading to self-destruction. This process is essential during multicellular development, organ morphogenesis, tissue homeostasis and immuno-defence against infected or damaged cells (Vila *et al.*, 2003). The death of cells by PCD is often marked by a series of morphological changes such as cell shrinkage, membrane blebbing, nuclei condensation and then fragmentation, releasing small membrane-bound apoptotic bodies (Lodish *et al.*,2000). So the term PCD is often referred to as "apoptosis", a

Greek word that means "falling off" as in leaves from a tree, although apoptosis is just one morphological form of PCD. In contrast to necrosis which is defined by cell swelling and bursting, releasing intracellular contents which may damage surrounding cells and often cause inflammation, apoptotic cells do not release constituents into extracellular milieu. The generated small apoptotic bodies are generally phagocytosed by other cells. So PCD normally serves as a safe way to clear unneeded cells in multicellular organisms. In the mammalian nervous system, PCD controls the number of neurons as the majority of nerve cells generated during development also die by PCD during development. However, under pathological conditions, PCD may contribute to the nerve cells loss in neurodegenerative diseases such as Alzheimer's disease. A β, the central molecule in AD was shown to directly induce apoptosis of cultured neurons and inhibition of particular members of the caspase family has been reported to partially or completely protect cells against A β -induced apoptosis in vitro. So research of PCD in AD may help to understand the reason of nerve cell loss in AD brains and even find ways to prevent and cure the disease.

1.8 Objectives of the present study

Cdk5/p35^{nck5a} is one of the candidates responsible for the hyperphosphorylation of tau protein which is the main component of the AD hallmark, neurofibrillary tangles. Under neurotoxic conditions, p35 is cleaved to p10 and p25. While p35 and p25 have

received intensive studies on their functions and relationships with AD, the role of p10 is little understood.

So the main object of the present study was to explore the influence of p10 overexpression on the mammalian cells. All the materials and methods used are listed in Chapter 2 and Appendices. Chapter 3 focuses on the work of plasmids amplification which serves as preparatory work for p10 overexpression study. Then, Chapter 4 explores the influence of p10 overexpression on different mammalian kidney cells including Cos-7 and HEK293. Subsequently, Chapter 5 further examines the influence of p10 overexpression on neuronal cells. Finally, the significance of my research and future work are discussed in Chapter 6.

CHAPTER TWO

MATERIALS AND METHODS

2.1 Materials

2.1.1 Media

All culture media used are listed in Appendix A. Culture media and serums were kept in 4˚C fridge respectively for long-term storage. The amount of serum was calculated and mixed with culture medium freshly immediately before each experiment.

2.1.2 Bacteria and Mammalian cell lines

Escherichia coli:

The competent E.coli for transformation was kept in -80˚C until usage. The detailed information of the E.coli used is listed in Appendix A.

Mammalian cell lines:

All the cell lines used were purchased from American Type Culture Collection (ATCC) and cultured in corresponding complete growth medium with 1% Penicillin Streptomycin at 37˚C, 5% CO_2. For long-term storage, cells were suspended in corresponding complete growth medium with 5% (v/v) DMSO and kept in liquid nitrogen. All subculture and cell treatment experiments were performed in a Bio-Hazard Class II hood (Gelman, 1892-02) to prevent bacteria contamination.

a. Cos-7 (ATCC, CRL-1651)

Complete growth medium: DMEM with 10% fetal bovine serum

b. HEK293 (ATCC, CRL-1573)

Complete growth medium: DMEM with 10% fetal bovine serum

c. PC12 (ATCC, CRL-1721)

Complete growth medium: DMEM with 10% fetal bovine serum and 5% horse serum

Differentiation growth medium: DMEM with 1% fetal bovine serum and 0.5% horse serum

d. Neuro-2a (ATCC, CCL-131)

Complete growth medium: DMEM with 10% fetal bovine serum

2.1.3 Cell culture conditions

The mammalian cells were grown as monolayer in 25 cm^2 polystyrene flasks in complete growth medium with 1% Penicillin Streptomycin in a 37˚C incubator with a water-saturated 5% CO_2 condition.

2.1.4 Plasmids

The plasmids used are listed in Appendix B. All original and amplified plasmids were stored in TE buffer at -20˚C.

2.1.5 Solutions and Kits

All solutions and Kits used are listed in Appendix C.

2.1.6 Other materials

Information of all other materials is mentioned in the "Methods" section.

2.2 Methods

2.2.1 Bacteria transformation

For each transformation, a tube of DH5- α E.coli solution was taken out from -80˚C and thawed on ice. During the waiting period, the water bath was turned on and set to stable at 42˚C. Meanwhile, a 14 ml round bottom Falcon tube (BD Falcon, 352057) was pre-chilled in ice. When totally thawed, the bacteria solution was pipetted into the Falcon tube followed by addition of original plasmid (about 0.5μg). Then, the tube was incubated on ice for 30 minutes. After that, the tube was incubated in 42˚C water bath for 90 seconds to heat shock the bacteria followed by 2-minute incubation on ice. Next, 1ml LB broth was added into the bacteria-plasmid mixture and bacteria were cultured for 1 hour at 37˚C on a shaker (160-180 rpm). To get single colony, 50μl bacteria-plasmid mixture was spread onto an agar plate with antibiotics (1% agarose, 25-30μg/ml antibiotics) which subsequently was incubated overnight at 37˚C in a Biocell 1000 incubator (SPD Scientific Pte Ltd).

2.2.2 Small-scale plasmid extraction by GFX Micro Plasmid Prep Kit

For small-scale plasmid extraction, a single colony was picked up by a tooth pick and inoculated into 2ml LB broth containing antibiotics (about 25μg/ml). Then bacteria were left to grow overnight at 37˚C with shaking (180rpm). The next day, the overnight culture was transferred to a 14 ml Falcon tube and centrifuged at 14,000 rpm for 30 seconds to pellet bacteria. After supernatant was removed, 150μl of Solution I

was added in to suspend bacteria pellet by vortex. Until bacteria were totally suspended in Solution I, 150μl of Solution II was added in to lyse the bacteria. To avoid of breaking bacterial genomic DNA, solutions were mixed by inverting tubes gently instead of vortex. The mixture was incubated at RT for 3 minutes before adding 300μl of Solution III. After 3-minute incubation on ice the mixture was centrifuged at 14,000 rpm for 5 minutes. In this step, most of the cell components including proteins and genomic DNA were pelleted while plasmids remained in the supernatant. Subsequently, the supernatant was transferred to a GFX column and incubated at RT for 1 minute followed by centrifugation at 14,000 rpm for 30 seconds. The plasmids were supposed to bind in the column after this step. Next, the flow-thru was discarded and the column was washed once with 400μl wash buffer. After washing step, the column was centrifuged twice at 14,000 rpm for 1 minute to get rid of residual ethanol. To make sure the residual ethanol was removed completely, the column was air-dried by waving for 10 times. Then the column was transferred to a 1.5 ml tube followed by addition of 50μl of ddH$_2$O to dissolve the plasmids. The column was incubated at RT for 1 minute and centrifuged at 14K rpm for 1 minute. Finally, the DNA concentration was measured by a spectrophotometer (BioSpec-1601, Shimadzu Pte Ltd). As a rule of thumb, the yield of small-scale plasmid extraction is between 15μg-25μg for each plasmid. DNA solution was stored at -20˚C.

2.2.3 Large-scale plasmid extraction and purification by HiSpeed Plasmid Midi Kit

For large-scale plasmid extraction, the single colony was first inoculated into 5ml LB broth containing antibiotics (about 25μg/ml) and left to grow overnight at 37˚C with shaking (180rpm). The overnight culture was then transferred to 100 ml LB broth containing antibiotics (about 25μg/ml) and left to grow for about 10 hours at 37˚C with shaking (180rpm). After culture, the bacteria cells were pelleted by centrifugation at 4,000 rpm (JA14 as the rotor) for 10 min at 4˚C using Avanti J-20 XP centrifuge (Beckman Coulter). Then the supernatant was discarded and the bacterial pellet was resuspended in 6 ml Buffer P1. Until bacteria were totally suspended by vortex, Buffer P2 was added in and mixed gently but thoroughly by inverting the tube 4 to 6 times. The mixture was then incubated at RT for 5 minutes followed by addition of 6 ml pre-chilled Buffer P3 to lyse the cells. Again, the solutions should be mixed gently by inverting the tube 4 to 6 times instead of vortex. After the solutions were mixed thoroughly, the lysate was poured into the barrel of the QIAfilter Cartridge and incubated at RT for 10 minutes. During the waiting period, 4 ml Buffer QBT was added into a HiSpeed Midi Tip to equilibrate the column by gravity flow. When the incubation time was end, the cell lysate was filtered through the QIAfilter Cartridge and transferred into the equilibrated HiSpeed Midi Tip. Next, the cleared lysate was allowed to enter the resin by gravity flow. In this step, the plasmids were supposed to bind in the resin. Subsequently, the HiSpeed Midi Tip was washed by 20 ml Buffer QC before the plasmids were eluted with 5 ml Buffer QF. In the next step, DNA plasmids were precipitated by 3.5 ml room-temperature isopropanol for 5 minutes. During the

incubation period, a QIAprecipitator Midi Module was attach onto the outlet nozzle of a 20 ml syringe and placed over a waste bottle. Then the elute/isopropanol mixture was transferred into the 20 ml syringe and filtered through the Module using constant pressure. In this step, the plasmids were supposed to be further purified and bind in the QIAprecipitator Midi Module. After that, the Module was washed by 2 ml 70% ethanol and air-dried by pressing the air through the Module repeatedly. Before the next step began, the outlet nozzle of the QIAprecipitator should be dried with absorbent paper to prevent ethanol carryover. In the final step, Buffer TE was filtered through the Module to elute DNA plasmids into a 1.5 ml tube. This step was repeated once to ensure the maximum yielding amount. DNA concentration was measured by the spectrophotometer. As a rule of thumb, the yield of large-scale plasmid extraction is between 150μg-250μg for each plasmid. DNA solution was stored at -20˚C.

2.2.4 Restriction endonuclease digestion of the DNA plasmids (Table 2.1)

To perform restriction endonuclease digestion, the components showed in Table 2.1 were added into a 1.5 ml tube in the sequence from left to right. For EcoR I digestion, EcoR I buffer and EcoR I enzyme were required. For double digestion, besides EcoR I buffer and EcoR I enzyme, Not I enzyme was required. (The enzyme should be added the last and proceed immediately to the next step.) When all the components were added in, the digestion solution was incubated at 37˚C water bath for 1 hour. After completion, the solution should be subject to DNA electrophoresis immediately.

ddH$_2$O(μl)	plasmid(ng)	EcoR I buffer(μl)	Enzyme(u)	total(μl)
top to 10	500	1	5 to 6	10

Table 2.1 The components and amount required for restriction endonuclease digestion.

2.2.5 DNA gel electrophoresis

Seakem LE agarose (Cambrex, 50004) was mixed with about 50 ml TAE buffer and melt by a microwave for 1 minute (The amount of the agarose used was calculated according to the percentage of the gel. In my work, I used 1% or 1.5% gel). After melting, the agarose solution was poured into the DNA gel tray. About half an hour later the agarose solution was cool down and form agarose gel. Then about 200ng plasmids were mixed with 6X DNA loading buffer including Sybr-green forming 1X DNA loading solution which was subsequently loaded into the agarose gel. The DNA gel was run in Sub-Cell GT System (Bio-Rad, 170-4481) at 70 voltages for about 1 hour. After the end of the electrophoresis, the results were checked and photos were taken by ChemiGenius[2] System (SynGene Corp.). Finally, the data were analyzed by the software GeneSnap 6.03.

2.2.6 Subculture of the mammalian cell lines

When the confluence of the cell lines in the flask reached 90% or more, cells was subcultured to maintain their viability and normal features. Firstly, complete growth medium with 1% PS was prepared and 0.5% Trypsin solution was diluted 4 times with 1X PBS forming 0.125% Trypsin solution (For PC12 subculture, Trypsin is not

needed). Then the freshly prepared growth medium and PBS was warmed up to 37˚C in water bath. Next, original medium in the T-flask (Nunc, 156340) was removed and cells were rinsed with 6ml 1X PBS once. After removal of PBS, 1ml 0.125% Trypsin solution was added in and the cells were subject to Trypsin digestion at RT for 2-10 min until cells were not tightly attached to the flask bottom. Then 6 ml pre-warmed growth medium was added in and the cells were completely suspended by pipetting. Subsequently, 0.7ml or1.5ml cell suspension was aliquoted to a new flask and top up to 6ml with new growth medium. So the subculture ratio was 1:4 or 1:8. In some cases, cells were to be seeded into the multidishes for treatment. Then cell concentration would be measured by a hemacytometer (Sigma, Z359629) before seeding. At last, the new flask was maintained in the cell culture incubator (Binder Corp.) at the condition of 37˚C, 5% CO_2 until the next subculture.

2.2.7 Mammalian cell line transfection experiments

a. Transfection by FuGENE 6 (24 well plate)

Firstly, 1μl FuGENE 6 reagent was diluted in 100μl serum-free medium. Then 0.5μg DNA plasmid was added into diluted FuGENE 6 reagent. The mixture was incubated at RT for 20 minutes. In order to prevent antibiotics entering the cells and causing cell injury, cell medium was changed to anti-biotics free medium (500μl/well) before adding the FuGENE/DNA mixture into the wells (100μl/well). Finally, cells were incubated at 37˚C, 5% CO_2 for 24-48 hours.

b. Transfection by Gene Porter 2 (24 well plate)

Firstly, 5μl Gene PORTER 2 transfection reagent was diluted in 20μl serum-free medium. Meanwhile, 1μg DNA plasmid was diluted in 25μl DNA diluent and incubated at RT for 3 minutes. Then DNA solution was mixed with Gene PORTER 2 transfection reagent and the mixture was incubated at RT for 10 minutes. During this period, cell medium was changed to antibiotics-free medium (250μl/well). Next, DNA/Gene PORTER 2 mixture was added into the wells (50μl/well). Finally, cells were incubated at 37˚C, 5% CO_2 for 24-72 hours.

c. Transfection by GeneJammer (24 well)

Firstly, 3μl GeneJammer transfection reagent was diluted in 100 μl of sterile, room temperature, serum-free, antibiotics-free DMEM. The diluted solution was incubated at RT for 5 to 10 minutes. Then 1μg DNA plasmid was added in and the mixture was incubated at RT for another 5 to 10 minutes. During this period, the original medium in the wells was removed and replaced by150μl fresh serum-containing but antibiotics-free medium. Next, transfection mixture was added into the wells (100μl/well) and the whole plate was gently rocked for mixing. After that, the cells were incubated at 37˚C, 5% CO_2 for 3 hours before addition of 250μl/well serum-containing medium. Finally, the cells were incubated at 37˚C, 5% CO_2 for further 24-72 hours.

d. Transfection by MBS Mammalian Transfection Kit (24 well plate)

Firstly, DNA plasmid was diluted in ddH_2O forming 45μl solution in a 1.5 ml tube. Then 5μl solution 1 and 50μl solution 2 were added in and mixed. The mixture was incubated at RT for 10 to 20 minutes before transfection. During this period, the original medium was removed and replaced by medium with 6% solution 3 (500μl/well). Next, precipitate in the DNA suspension was resuspended by pipette and 50μl of the DNA suspension was slowly added into the wells in a dropwise manner. The plate was swirled once for mixing well. In the next step, the cells were incubated for 3 hours at 37c, 5% CO_2. After that, the medium was removed and replaced by complete growth medium without antibiotics. Finally, the cells were incubated at 37˚C, 5% CO_2 overnight.

e. Transfection by TransIT-Neural Transfection Reagent Kit (24 well plate)

In the first step, 1μl TransIT-Neural Reagent was diluted in 100μl OPTI-MEM. The diluted solution was incubated at RT for 5 minutes. Then 0.5μg DNA plasmid was added in and mixed by gentle pipetting. Subsequently, the reagent-DNA mixture was incubated at RT for 10 minutes. After the incubation, the transfection solution was added into the wells (100μl/well) and the plate was gently rocked for mixing. At last, the cells were incubated at 37˚C, 5% CO_2 for 24-48 hours.

f. Transfection by Lipofectamine 2000 (24 well/ 6 well plate)

Firstly, complete growth medium without PS was prepared (500μl/24 well, 2ml/6 well) and warmed up to 37˚C in water bath. Then 1μl Lipofectamine reagent was diluted in 50μl OPTI-MEM for each 24 well or 4μl Lipofectamine reagent was diluted in 250μl OPTI-MEM for each 6 well. Then diluted solution was incubated at RT for 5 minutes. Next, 1μg DNA plasmid was diluted in 50μl OPTI-MEM for each 24 well or 4μg DNA plasmid was diluted in 250μl OPTI-MEM for each 6 well. The diluted DNA solution was incubated at RT for 3-5 minutes. After that, the two diluted solution was mixed together and incubated at RT for 20 minutes. During this period, the cell medium was changed to complete growth medium without antibiotics (500μl/ 24 well or 2ml/6 well). When the reagent-DNA mixture was ready, it was added into the wells directly (100μl/ 24 well, 500μl/ 6 well). Then the cells were incubated for indicated time at 37˚C, 5%CO_2. For kidney cell lines, medium with transfection reagent was removed and replaced by complete growth medium without antibiotics the next day. For neuronal cell line, medium with transfection reagent was removed and replaced by complete growth medium without antibiotics 3 hours after adding transfection reagent because neuronal cells were more sensitive to the transfection reagent.

g. Transfection by Transfectin reagent (24 well and 6 well plate)

Firstly, 1 μg DNA plasmid was diluted in 50 μl of DMEM for each 24 well or 4μg DNA plasmid was diluted in 250 μl of DMEM for each 6 well. Then 1 μl Transfectin lipid reagent was diluted in 50 μl of DMEM for each 24 well or 4 μl Transfectin lipid

reagent was diluted in 250 µl of DMEM for each 6 well. For high transfection efficiency, polystyrene tubes (BD Falcon, 352054) were used to hold Transfectin lipid reagent. Next, the diluted DNA and the diluted Transfectin lipid reagent were combined together and incubated at RT for 20 minutes to allow DNA-Transfectin lipid reagent complexes to form. Subsequently, the DNA-Transfectin lipid reagent complexes (100 µl/24 well or 500 µl/6 well) were added directly into each well. The plate was rocked gently for mixing. To ensure the interaction of the complexes with the cells at the bottom, the whole plate was centrifuged at 1000 rpm for 5 minutes by Eppendorf centrifuge 5810R (B. Braun Singapore Pte Ltd). Finally, the cells were incubated for indicated time at 37°C and 5% CO_2. For kidney cell lines, medium with transfection reagent was removed and replaced by complete growth medium without antibiotics the next day. For neuronal cell line, medium with transfection reagent was removed and replaced by complete growth medium without antibiotics 3 hours after adding transfection reagent.

2.2.8 Harvest cells in 6-well plate for Western-blot using RIPA buffer method

At indicated time after transfection, the cells were harvested for Western-blot analysis. Specifically, the growth medium was removed and pre-chilled RIPA buffer was added (150µl/well). The cells were then scraped down in RIPA buffer completely and cell lysate was stored at -20˚C overnight. The next day, cell lysate was thawed on ice and centrifuged at 13k rpm for 15 minutes at RT by Micro Centaur Centrifuge (SANYO). Then the supernatant was carefully transferred to a fresh tube and stored at -20˚C or -

80˚C. On the other hand, 25μl of 5X SDS loading buffer with β-mercaptoethanol was added into each pellet and mixed by vortex. The pellet sample was then heated at 100˚C for 10 minutes and stored at -20˚C or -80˚C.

2.2.9 Determine protein concentration of the samples in RIPA buffer

Before Western-blot analysis, the protein concentration should be measured by RC DC protein assay kit. Firstly, 5 μl of DC Reagent S was added to each 250μl of DC Reagent A forming Reagent A'. Then a protein standard for the standard curve was prepared as shown in Table 2.2. Subsequently, 25 μl of each standard and sample was added into the microfuge tubes. Then 125 μl RC Reagent I was added into each tube and mixed by vortex. The tubes were incubated at RT for 1 minute. Next, 125 μl RC Reagent II was added into each tube and mixed by vortex. The tubes are centrifuged at 13K rpm for 10 minutes. Then the supernatant was discarded followed by addition of 127 μl Reagent A' to each tube. The tubes were incubated at RT until precipitate was completely dissolved. In the next step, the tubes were vortexed and 1ml of DC Reagent B was added into each tube. Then the tubes were vortexed again immediately and incubated at RT for 15 minutes. Finally, the absorbance at 750nm was read by the spectrophotometer (Beckman, DU 640B).

RIPA buffer (μl)	10mg/ml BSA (μl)	protein standard (μg/μl)
100	0	0.0
95	5	0.5
90	10	1.0
85	15	1.5
80	20	2.0

Table 2.2 Protein standard is prepared from BSA (10mg/ml) and RIPA buffer freshly.

2.2.10 SDS-PAGE and Western-blot analysis

The samples were denatured by heating at 100˚C for 5 minutes and mixed with 5X SDS loading buffer with β-mercaptoethanol forming 1X protein solution. Then the samples and protein standard were stacked and resolved by SDS-PAGE. After that, proteins were transferred from gel to PVDF membrane in transfer buffer. The blot was then blocked in 10 ml blocking buffer. After the TBST washing steps the blot was incubated in desired primary antibody and secondary antibody. Finally, the blot was incubated in chemiluminescent substrate (West Femto or West Pico, Pierce) according to manufacturer's instructions and chemiluminescence was detected by ChemiGenius[2] System (SynGene Corp.) and data were analyzed by the software GeneSnap 6.03.

2.2.11 Immunohistochemistry and DNA staining by Hoechst 33342 (24 well)

About 48 hours after transfection experiment, the medium was removed and 4% paraformaldehyde (300μl/ well) was applied to fix the cells for 20 minutes at RT. Cells were then rinsed with PBS thrice (300μl/well) and treated with100mM NH_4Cl (250μl/well) at RT for 1 minute. Cells were rinsed with PBS thrice again and incubated with 0.2% Triton-X 100 (250μl/well) at RT for 30 minutes to permeate the cell membrane. After removal of Triton-X 100, cells were blocked in 10% goat serum (250μl/well) for 1 hour followed by primary antibody (anti-cmyc, 1:250 in goat serum, 250μl/well) at 4˚C overnight. The next day, primary antibody was removed and cells were rinsed by PBS thrice followed by secondary antibody (goat-anti-rabbit, 1:2000 in goat serum, 250μl/well). After 2 hour incubation, cells were rinsed by PBS thrice and

nuclei were stained by Hoechst 33342 solution (5μg/ml) at RT for 10 minutes. Finally, results were checked and fluorescence photos were taken by a fluorescence microscope (Leica DM IRB). Data were analyzed by the software: Leica QFluoro.

2.2.12 Harvest cells in 6-well plate for FACS analysis

At indicated time after transfection, cells were harvested for FACS analysis. Firstly, a tube with 4.5 ml 70% ethanol was chilled in ice. Then the cell medium was carefully removed and cells were totally suspended in PBS (2ml/well). Subsequently, cell suspension was transferred to 15ml tube and centrifuged at 300X g-500X g for 5 minutes. Next, cells were resuspended in PBS (0.5ml/tube) and transferred to pre-chilled 70% ethanol. In order to fix the cells thoroughly, the cell fixative solution was stored at -20˚C overnight. The next day, the tubes were centrifuged at 300X g-500X g for 5 minutes and supernatant was discarded. Then the cell pellet was washed with PBS (2ml/tube) and tubes were centrifuged again at 500X g for 5 minutes. After the supernatant was discarded, cell pellet was resuspended in PI staining solution with RNase (500μl /tube) and DNA was stained by PI. In order to reduce the cell clumps, cell suspension was filtered through a 22-gauge needle and then incubated at RT for 30 minutes. At last, FACS analysis was performed by a flowcytometer machine (Beckman Coulter, Elite cytometer) and data were analyzed by the software: WinMDI 2.8

2.2.13 PC12 differentiation experiment

Before cell seeding, the plates were coated with Poly-D-Lysine (0.1mg/ml, 500μl/well) and incubated at 37˚C overnight. The next day, Poly-D-Lysine solution was removed and wells were washed with Milli-Q water (500μl/well) once. After removal of the Milli-Q water, the plates were air-dried in the hood. When the plates were ready for seeding, PC12 cells were suspended in differentiation growth medium with 100ng/ml NGF and seeded into the coated plates (300μl/24 well or 1.5ml/6 well). Finally the cells were incubated at 37˚C, 5% CO_2. For differentiation experiment performed after transfection, about 24 hours after transfection the culture medium was changed to differentiation growth medium with NGF (100ng/ml) and the incubation of cells were continued at 37˚C, 5% CO_2.

2.2.14 Statistical analyses

The unpaired Student's t-test was performed to determine the statistical significance of difference. A probability (p) value of less than 0.05 was considered as statistical significance.

CHAPTER THREE

AMPLIFICATION OF THE PLASMIDS

3.1 Introduction

The present study sought to explore the influence of overexpression of p10, a 98-amino-acid protein, on different mammalian cells which required the delivery of p10 cDNA into the cells. To achieve this goal, two different plasmids were chosen as the vehicles and the plasmids with the p10 cDNA insert were engineered by Dr. Robert Qi's group (UST, Hongkong) and sent to me as a gift.

The first plasmid named as pEGFP-N3 vector encodes a red-shifted variant of wild-type GFP as a reporter which has been optimized for brighter fluorescence and higher expression in mammalian cells (refer to Appendix B for more information). Moreover, the pEGFP-p10 plasmid was generated by inserting the p10 cDNA at the C-terminus of GFP gene. The second plasmid called pCI-neo-myc mammalian expression vector was modified from pCI-neo vector by engineering two myc tags between two restriction sites, Sal I and Not I (refer to Appendix B for more information). The myc tag encodes eleven amino acids which is only 1.2 KD and can be expressed in different protein contexts and still be recognizable. So it is now widely used in western-blot technology, immunoprecipitation, and flowcytometry and therefore very useful for monitoring expression of recombinant proteins in bacteria, insect cells and mammalian cells (Terpe, 2003). In addition, the pCI-p10-myc plasmid was constructed by inserting the p10 cDNA between two restriction sites, EcoR I and Sal I.

However, the amount of original plasmids available was just several micrograms each which were far less than the required amount for transfection experiments. So the original plasmids should be amplified as the preparatory work for p10 overexpression studies. In this work, the bacteria E. coli served as the plasmid transformation and amplification host. And HiSpeed Plasmid Midi Kit was applied for the plasmids extraction and purification. In order to estimate the amplification accuracy, endonuclease digestion and DNA electrophoresis were also included in the work.

In summary, the present chapter aimed at the amplification of the four original plasmids including pEGFP-N3 vector, pEGFP-p10, pCI-neo-myc vector, and pCI-p10-myc. Once amplified, the four plasmids would be delivered into different mammalian cells for overexpression experiments.

3.2 Results and Discussion

3.2.1 Bacteria transformation

E. coli strain DH5 α served as the host for plasmids amplification (refer to Appendix A for more information). About 0.5μg original plasmid each was used for transformation of bacteria and the transformation experiment was carried out according to the method described in 2.2.1. Transformed bacteria solution was spread on agar plate and cultured at 37˚C overnight with Kanamycin as selection marker for pEGFP plasmids and Ampicilin for pCI plasmids. The next day, about several decades of bacteria single colonies appeared sporadically throughout the agar plate suggesting that the transformation efficiency ranged over 500-1000 transformants/μg DNA.

3.2.2 Bacteria culture

Single colonies of transformant were picked up and cultured in LB broth with antibiotics (25-30μg/ml) at 37˚C on shaker (about 180rpm). The bacteria growth status was estimated by checking the turbidity of bacteria culture solution. At the beginning, the bacteria culture solution was almost transparent. Bacteria culture was considered complete and ready for plasmids extraction and purification when culture solution was opaque which generally took about ten hours.

3.2.3 Plasmids extraction and purification

Plasmids were mainly extracted and purified by HiSpeed Plasmid Midi Kit according to the method described in 2.2.3. Normally DNA concentrations were between 0.15mg/ml to 0.25mg/ml and total DNA yielded was between 150μg to 250μg for each plasmid.

3.2.4 Digestion of the plasmids by EcoR I and DNA electrophoresis

To compare the size of the original plasmids with the amplified ones, EcoR I restriction enzyme was used to cut all the plasmids at the single site: $A^{630}A^{631}T^{632}T^{633}$ followed by DNA electrophoresis. As already known, pEGFP-N3 vector is 4.7 KB at length and p10 cDNA insert is about 300 base pairs. So theoretically, pEGFP-p10 is about 5 KB. The DNA electrophoresis after EcoR I digestion revealed that original pEGFP plasmids and corresponding amplified ones were about the same size and the sizes of the plasmids were totally consistent with theoretical ones (Fig3.1). On the other hand, pCI-neo-myc vector is 5.4 KB at length and pCI-p10-myc 5.7 KB theoretically. The results matched quite well with theoretical ones suggesting both the correctness of the plasmids and accuracy of the amplification process (Fig 3.2).
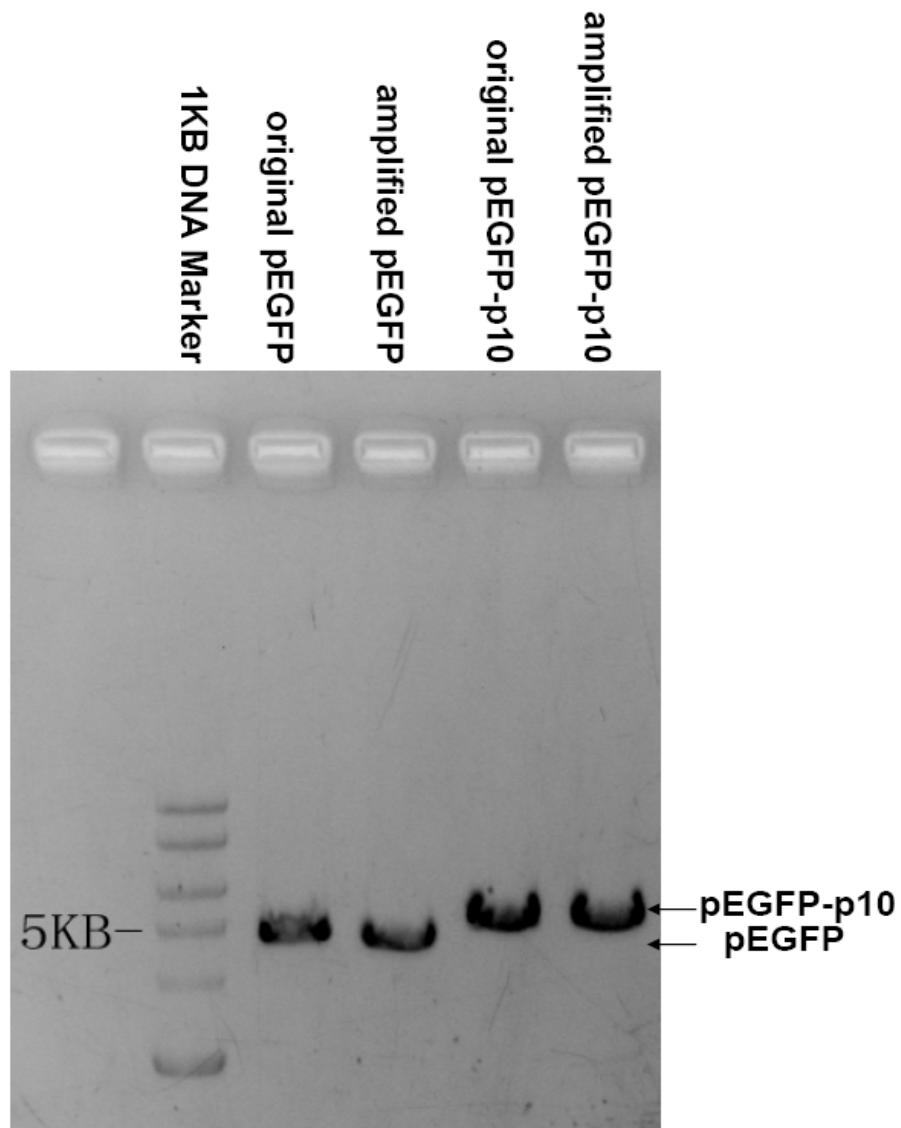
Figure 3.1 DNA gel showing original and amplified pEGFP plasmids digested by restriction enzyme EcoR I. DNA was stained by SYBR Green and the position of the plasmids is indicated by the black arrows on the right. A 1KB DNA marker on the left line shows that the sizes of the plasmids are correct.
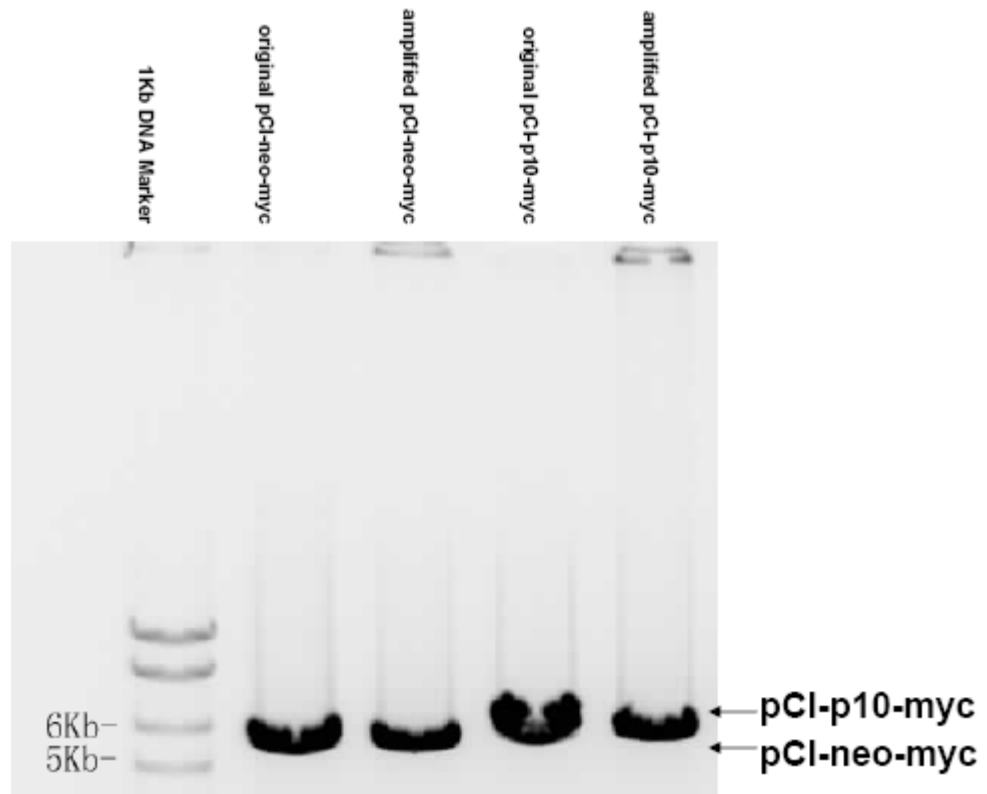
Fig 3.2 DNA gel showing original and amplified pCI plasmids digested by restriction enzyme EcoR I. DNA was stained by SYBR Green and the position of the plasmids is indicated by the black arrows on the right. A 1KB DNA marker on the left line shows that the sizes of the plasmids are correct.

3.2.5 Double digestion of pCI plasmids by EcoR I and Not I followed by DNA electrophoresis

To further confirm that the amplified pCI-p10-myc contained the p10 cDNA at the proposed site, amplified pCI-neo-myc vector and pCI-p10-myc were double digested by EcoR I and Not I. The plasmids before and after double digestion were subject to electrophoresis on a DNA gel together (Fig 3.3). Notably, after double digestion, pCI-p10-myc released a DNA fragment about 400 base pairs according to the 100bp DNA marker. As a control, the pCI-neo-myc vector released no DNA fragment after double digestion suggesting that the DNA fragment released by pCI-p10-myc could not be part of the vector. Moreover, there were about 100 base pairs between EcoR I and Not I in the pCI-neo-myc vector (refer to Appendix B for the vector information). p10 cDNA was about 300 base pairs. Theoretically the DNA fragment released after double digestion should be about 400 base pairs which matched with the result perfectly. By the way, it turned out that after digestion the vector ran slower than itself before digestion. The reason may be that before digestion the vector existed as a super coil plasmid while after digestion it was cut at two sites and turned into a more lineated form which ran slower than the super coil form in the agarose gel.

In summary, the result confirmed that the amplified pCI-p10-myc plasmid contained the p10 cDNA at the proposed site.
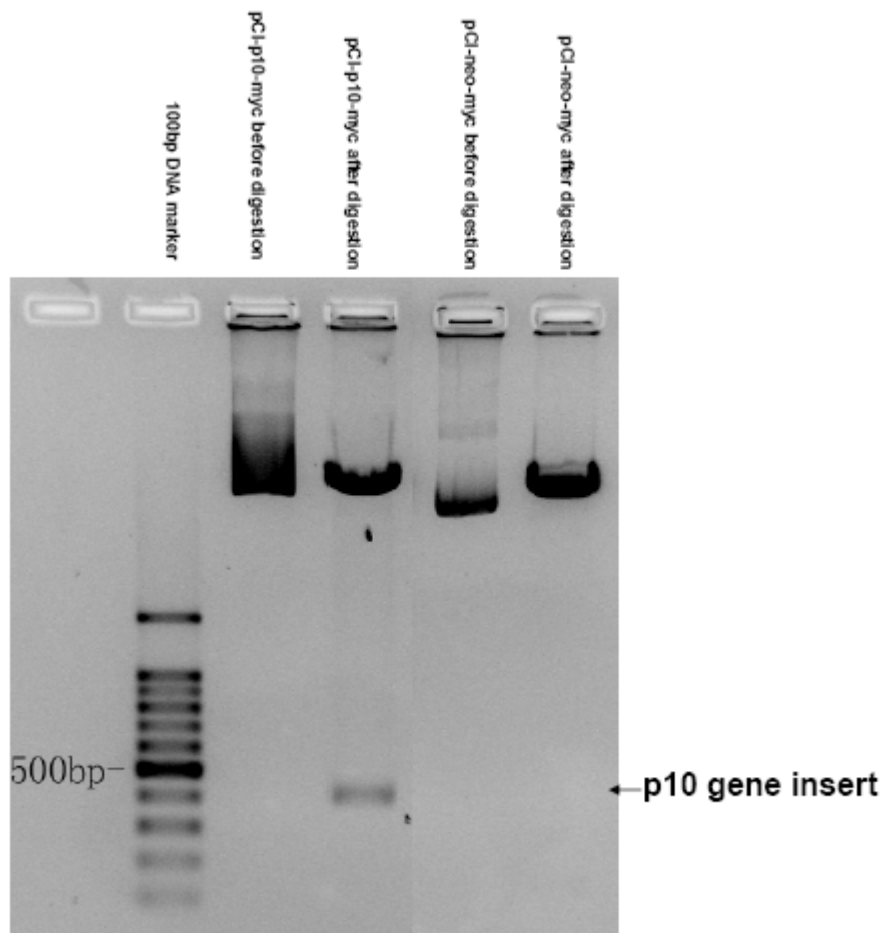
Fig 3.3 DNA gel showing the pCI plasmids before and after double digestion by EcoR I and Not I. p10 gene insert was released after double digestion while pCI-neo-myc vector released no DNA fragment.

3.3 Conclusion

The four plasmids including pEGFP-N3, pEGFP-p10, pCI-neo-myc and pCI-p10-cmyc were amplified from several micrograms to about two hundred micrograms. The amplification may be accurate shown by restriction enzyme digestion and DNA electrophoresis.

CHAPTER FOUR

OVEREXPRESSION OF p10 MEDIATES
DEATH OF KIDNEY CELLS

4.1 Overexpression of GFP-p10 mediated death of Cos-7 cells

4.1.1 Introduction

To deliver genes into the cells and make them expressed, generally there are two sorts of methods: recombinant virus-based technologies and non-viral transfection methods. Compared to virus-based technologies, non-viral transfection methods have the advantage of easier to use, less toxic, and not constrained to delivering plasmids below a relatively small size. However, it is well-known that the transfection efficiency of postmitotic neurons by non-viral method is quite low (Washbourne and McAllister, 2002). Moreover, to examine the influence of overexpression of p10 in mammalian cells, high transfection efficiency is required. At the first stage of present study, Cos-7 was chosen as the p10 overexpression host. Cos-7 is a cell line derived from CV-1 cell line by transformation with an origin defective mutant of SV40 which codes for wild-type T antigen. It is a kidney cell line from African green monkey and an optimal transfection host.

To obtain the highest transfection efficiency, altogether six transfection kits were tested which included Lipofectamine 2000, TransIT-Neural, GeneJammer, GenePORTER 2, MBS Mammalian Transfection Kit and FuGENE 6. Among them Lipofectamine 2000 was found to achieve the highest transfection efficiency (about 25%-30%) in Cos-7 together with low cytotoxicity, so this kit was selected to perform all the transfection experiments in subsequent work unless specially indicated. Lipofectamine 2000 reagent is a cationic lipid. When mixed with DNA, it interacts with the negatively charged

phosphate backbone of DNA to form the DNA-lipid complex which is capable of passing through the cell membrane. Thus Lipofectamine 2000 reagent serves as a vehicle for DNA to enter the nuclear for expression.

4.1.2 Results

4.1.2.1 48 hours after transfection, GFP-p10 fusion proteins were overexpressed in Cos-7 cells

About 48 hours after transfection, cells were harvested in RIPA buffer. Protein concentration of each sample was determined by RC DC Protein Assay Kit. 30 μg proteins of each sample were loaded into SDS-PAGE gels and the final results were shown in Fig 4.1. Altogether four antibodies were used in this experiment. The anti-GFP antibody recognized the epitope on the GFP protein. In Fig 4.1A, no band was detected in non-transfection sample while GFP bands appeared in vector control samples. Meanwhile, a GFP band and a 37KD GFP fusion protein band appeared in pEGFP-p10 sample. In Fig 4.1B, anti-n20-p35 antibody which recognizes the N-terminal region of p35 detected no band in either non-transfection sample or vector control sample while a band appeared at the same position as that of the GFP fusion protein band in Fig 4.1A. This confirmed that the 37KD band in pEGFP-p10 sample stood for the band of GFP-p10 fusion protein. Moreover, an anti-c19-p35 antibody which recognizes the C-terminal region of p35 did not detect any band as expected (Fig 4.1C). Finally, an anti-α-tubulin antibody was used to confirm that there were about equal amount of protein in each line (Fig 4.1D).
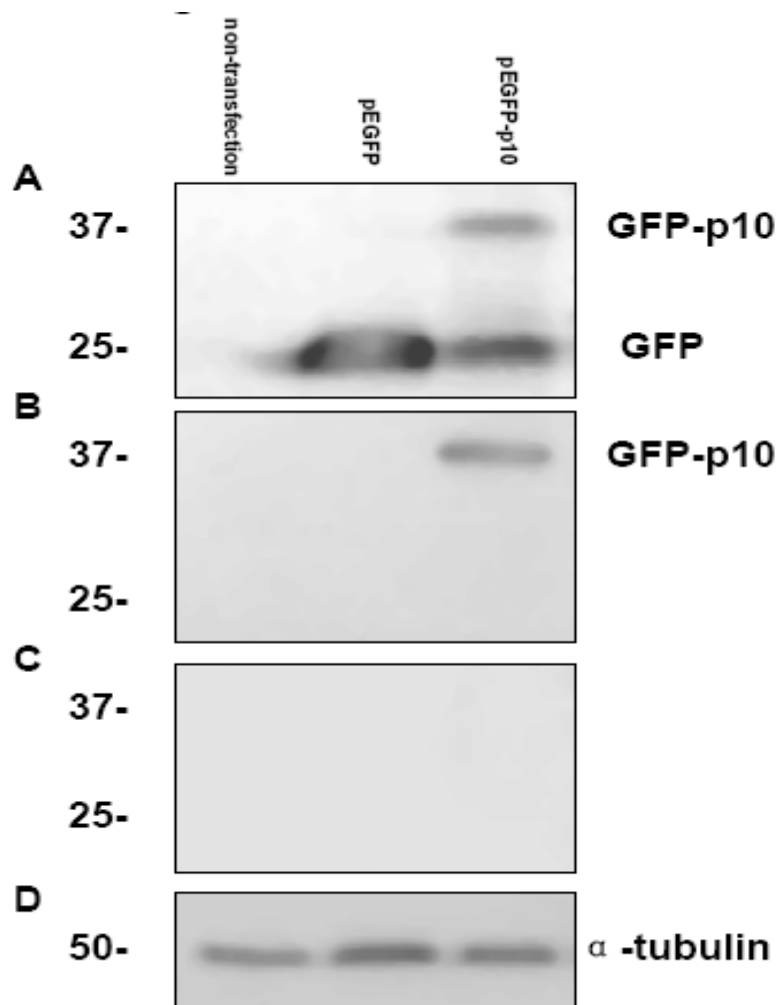
Fig 4.1 Western-blot analysis of the expression of the pEGFP plasmids in Cos-7 cells using (A) anti-GFP, (B) anti-n20-p35, (C) anti-c19-p35 and (D) anti-α-tubulin as internal control.

4.1.2.2 GFP-p10 overexpression in Cos-7 caused the change of whole cell morphology
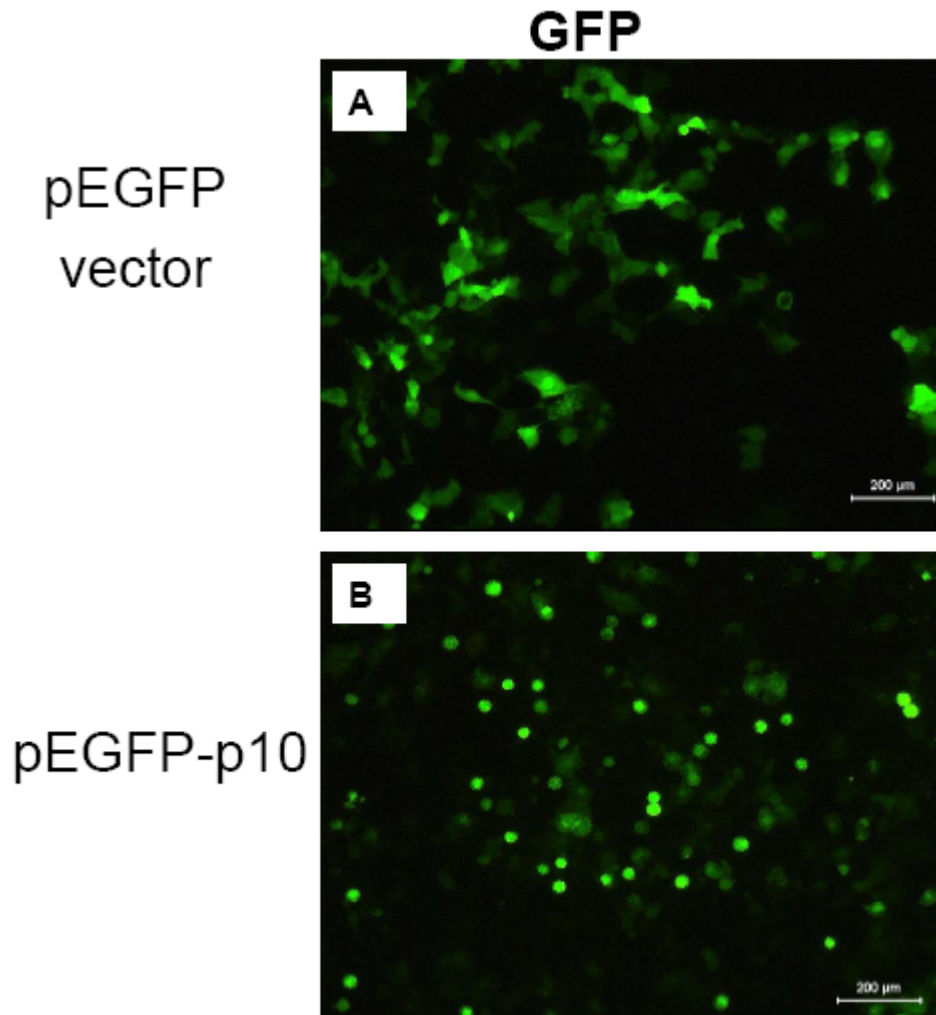

Fig 4.2 The change of GFP-p10 expressing cell morphology shown by GFP green fluorescence photos about 48 hours after transfection of Cos-7 with (A) pEGFP-N3 vector control and (B) pEGFP-p10.

While the morphology of Cos-7 overexpressing GFP vector control appeared normal, those overexpressing GFP-p10 displayed obvious abnormal whole cell morphology as shown in Fig 4.2. Cos-7 is a fibroblast-like cell line with obvious lamellipodia and is

adherent to the tissue culture plate (Fig 4.2A). But most of the cells expressing GFP-p10 shrank and displayed round cell morphology. Some even lost attachment to the plate (Fig 4.2B). These phenomena suggested that the expression of GFP-p10 in Cos-7 cells may disrupt cytoskeleton system and subsequently change the whole cell morphology. Moreover, the intensity of the abnormal morphology phenotype corresponded to the intensity of the GFP fluorescence suggesting that the cell morphology may also be influenced by the GFP-p10 expression level.

4.1.2.3 Cos-7 overexpressing GFP-p10 also displayed abnormal nuclei which indicated that they were probably undergoing apoptosis

To confirm those small round cells with GFP-p10 were really unhealthy or even dead, 48 hours after transfection cells were fixed by 4% paraformaldehyde and nuclei were stained by the DNA dye, Hoechst 33342. In Fig 4.3, vector expressing cells showed normal nuclei morphology while those overexpressing GFP-p10 showed obvious abnormal nuclei such as nuclei deformation, condensation and fragmentation (Fig 4.3D). As DNA fragmentation is one of the features of apoptosis, this result suggested that overexpression of GFP-p10 may lead to apoptosis.
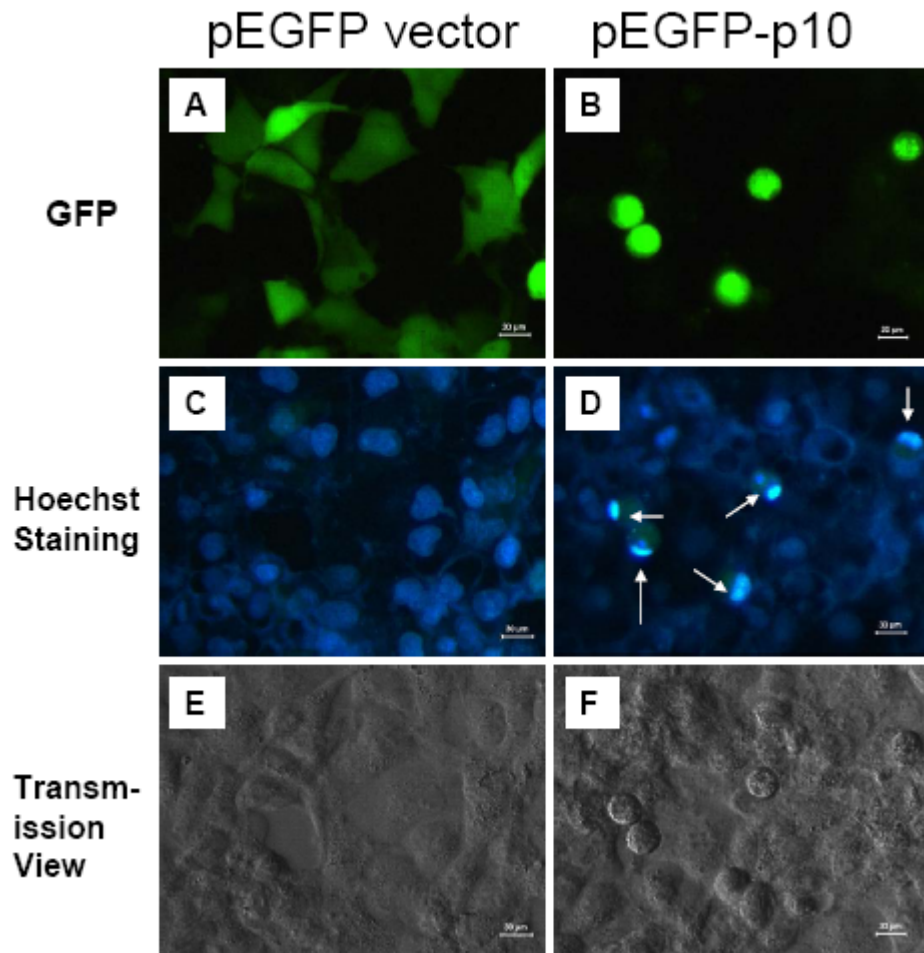
Fig 4.3 The abnormal nuclei of Cos-7 cells overexpressing GFP-p10 shown by fluorescence photos with higher magnification than those in Fig 4.2. Cells transfected with pEGFP-N3 vector control are shown in (A), (C), (E) from the same view while cells transfected with pEGFP-p10 are shown in (B), (D), (F) from the same view. White arrows in (D) indicate the abnormal nuclei which appear deformed, condensed or fragmented.

4.1.2.4 Abnormal nuclei rate of GFP-p10 expressing cells was significantly higher than that of GFP expressing cells
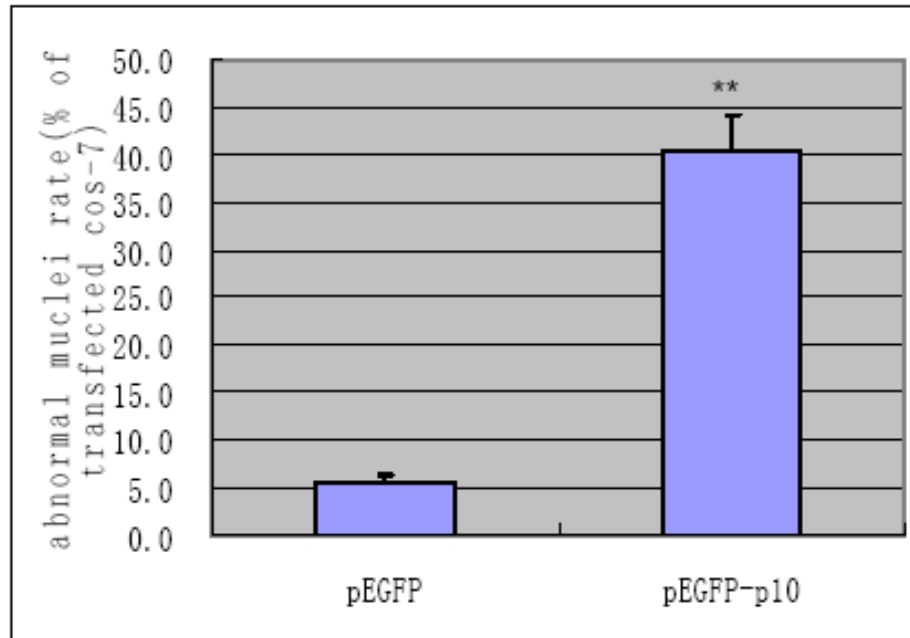

Fig 4.4 Cells expressing GFP-p10 displayed significantly higher abnormal nuclei rate than those expressing GFP alone.

Abnormal nuclei rate assay was performed on the cells expressing pEGFP and pEGFP-p10. Only GFP fluorescence positive cells were counted and nuclei were scored as abnormal only when nuclei appeared fragmented or condensed or deformed together with abnormal cell morphology as shown in Fig 4.3B. Values were mean±s.d. of three independent experiments. At least 300 cells were counted for each value. One-side student T test was done and **$p<0.01$ comparing to vector control. About 40% of the cells expressing GFP-p10 displayed abnormal nuclei which was about eight times that of the cells expressing GFP alone suggesting the high toxicity of p10 to Cos-7 cells.

4.1.2.5 FACS analysis revealed higher cell death rate in cells subject to pEGFP-p10 transfection than those subject to vector control transfection

To further assess the cell death rate, the flow cytometry technique was applied on FACS (Fluorescence Activated Cell Sorter) analysis. For active proliferating cells like Cos-7, normally all the cells are in the four phases of cell cycle: G1, S, G2 and M. The DNA amount in a single G1 cell is close to each other for the same cell type. When G1 cells enter S phase, the DNA amount increases continuously until cells reach G2 phase in which cells double the DNA amount. As shown in Fig 4.5A, the X axis stands for the DNA amount in a single cell and Y axis stands for the number of the cells. As G1 and G2 are long, and the amount of the DNA in these two phases is stable two peaks appears in the Fig 4.5A standing for G1 and G2 cells. When cells die by apoptosis, small DNA fragments are generated and tend to leak out of the cell after fixation and membrane permeation. In FACS analysis the cells with less DNA amount than G1 cells are called subG1 cells which are scored as dead cells.

Comparing panel (A) and (B) in Fig 4.5, cell death rate was a little higher among Cos-7 cells subject to pEGFP-p10 transfection than that of those subject to vector control transfection. This difference seemed to be contributed by the small peak in subG1 field as highlighted in the ellipse in Fig 4.5B. This suggested the increased DNA fragmentation rate among the cells subject to pEGFP-p10 transfection. Values in Fig 4.5C were mean±s.d. of three independent experiments. Ten thousand cells were counted for each value. One-side student T test was done and *$p < 0.05$ comparing to vector control.
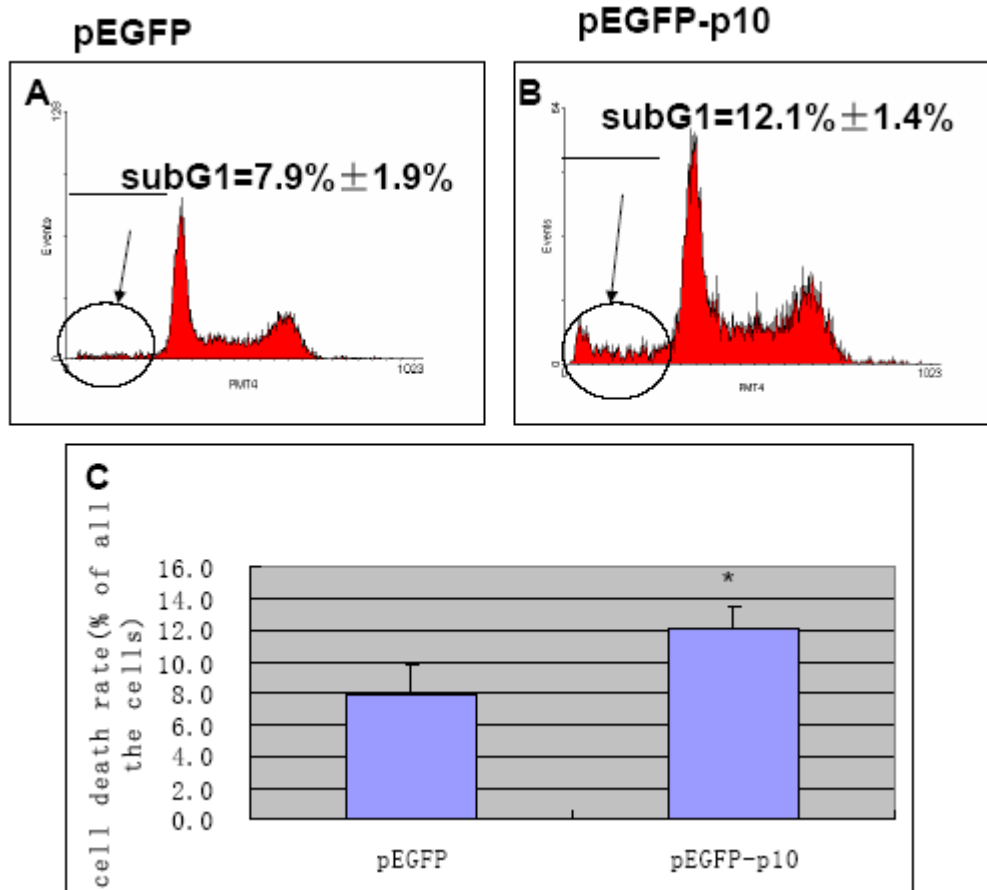
Fig 4.5 FACS analysis of the cell death rate. Panel (A) and (B) show the representative FACS pictures of Cos-7 cells subject to pEGFP-N3 and pEGFP-p10 transfection respectively.

4.1.3 Discussion

In this stage, evidence was collected that overexpression of GFP-p10 mediated toxic effect to Cos-7 cells by impairing the integrity of the cytoskeleton and probably inducing apoptosis. Compared to vector control, overexpression of GFP-p10 changed both the whole cell and nuclei morphology significantly as revealed by Fig 4.2-Fig 4.5.

By the way, there seems to be a discrepancy between the data in Fig 4.4 and Fig 4.5 as the abnormal nuclei rates differ about 35% in immunocytochemistry cell counting while the death cell rates only differ about 5% using FACS. Actually this is explainable. In abnormal nuclei rate assay only GFP positive cells were counted while in FACS analysis all the cells including GFP negative cells were counted. The transfection efficiency in Cos-7 is about 20%-30% which means the subG1 difference revealed by FACS analysis should be multiplied by a coefficient around 5 to reveal the true difference between transfected cells. Moreover, a part of the cells overexpressing GFP-p10 showing deformed nuclei which would be scored in abnormal nuclei assay may not be scored in FACS analysis because the small DNA fragments may not have been generated yet. Taken the above two facts into consideration, it is assumed that the data in Fig 4.4 and Fig 4.5 are generally consistent with each other.

The results raise the possibility that p10 is a toxic protein to mammalian cells. If this can be confirmed and proved to be true, it may contribute in explaining the neuronal cell death in AD brains as during such abnormal environment p10 is a product as well as p25 by activation of calpain and cleavage of p35. p10 may play a role in neuronal cell loss in AD.

However, there are at least two alternative explanations to the toxicity of GFP-p10. First, GFP protein is 27KD and is larger than p10. When GFP fuses with p10, p10 may somehow change the conformation of GFP and it is possible that the newly formed GFP contributes to the cytotoxicity instead of p10. Second, the attachment of GFP to the N-terminal of p10 may change the conformation of p10 protein. Possibly, it is the

new conformation of p10 which does not exist in vivo that is responsible for the cytotoxicity. So to rule out the above two possibilities, p10-cmyc fusion protein would be overexpressed in Cos-7 to check whether the same toxic effect would be generated.

4.1.4 Conclusion

Overexpression of GFP-p10 in Cos-7 cells generated abnormal whole cell and nuclei morphology suggesting apoptosis. However, whether the toxic effect was mediated by p10 needed to be confirmed by p10-cmyc overexpression in Cos-7 cells.

4.2 Overexpression of p10-cmyc also mediated death of Cos-7 cells

4.2.1 Introduction

As stated in the previous section, the GFP-p10 overexpression in Cos-7 cells mediated cell death but whether the toxic effect was due to the in vivo function of p10 protein remained a question. Two alternative explanations were put forward in 4.1.3. To rule out the alternative explanations and prove the toxic effect was really due to the function of p10, cmyc tag was applied to form the p10-cmyc fusion protein in Cos-7 by the same transfection method and condition. Compared to GFP tag, the cmyc tag had two advantages. First, the cmyc tag attached to the C-terminal of p10 which influenced the original structure of p10 less than the N-terminal tag. Second, the cmyc tag protein was

only 1.2 KD which was far smaller than the GFP protein (Terpe, 2003). This ensured the minimum influence of the tag to the structure and function of p10. So in this stage, the p10-cmyc fusion proteins were generated and expressed in Cos-7 cells to confirm the toxic effect of p10 protein.

4.2.2 Results

4.2.2.1 48 hours after transfection, p10-cmyc fusion proteins were overexpressed in Cos-7 cells

Cos-7 cells were subject to transfection and harvest. The protein concentrations of the samples were determined by RC DC protein assay. 20μg proteins of each sample were loaded into SDS-PAGE gels and the final results were shown in Fig 4.6. Altogether four antibodies were used in this experiment. Anti-cmyc antibody recognized the epitope of the cmyc tag. In Fig 4.6A, no band was detected in non-transfection Cos-7 samples. Unfortunately, the small myc band could not be seen in vector transfected samples because the myc protein was too small to be retained on PVDF membrane. But the band of p10-cmyc was clearly shown in pCI-p10-myc samples. This fusion protein band was confirmed by anti-n20-p35 antibody which recognized the N-terminal portion of p35 (Fig 4.6B). Moreover, an anti-c19-p35 antibody which recognized the C-terminal region of p35 did not detect any band as expected (Fig 4.6C). Finally, an anti-α-tubulin antibody was used to confirm that there were about equal amount of protein in each line (Fig 4.6D).
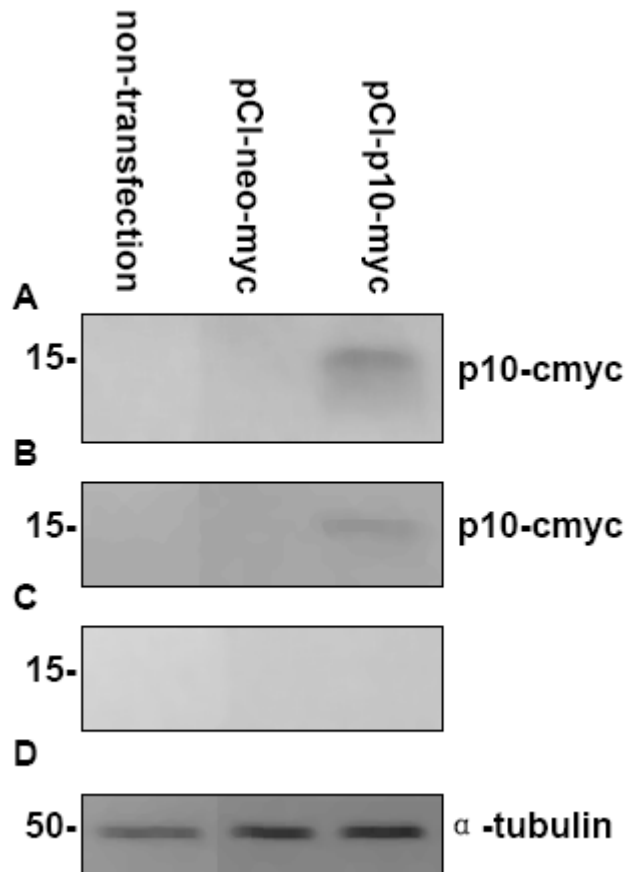
Fig 4.6 Western-blot analysis of the expression of the plasmids in Cos-7 cells using (A) anti-cmyc, (B) anti-n20-p35, (C) anti-c19-p35 and (D) anti-α-tubulin.

4.2.2.2 Cos-7 overexpressing p10-cmyc displayed both abnormal whole cell and nuclei morphology just like those observed in GFP-p10 overexpressing cells
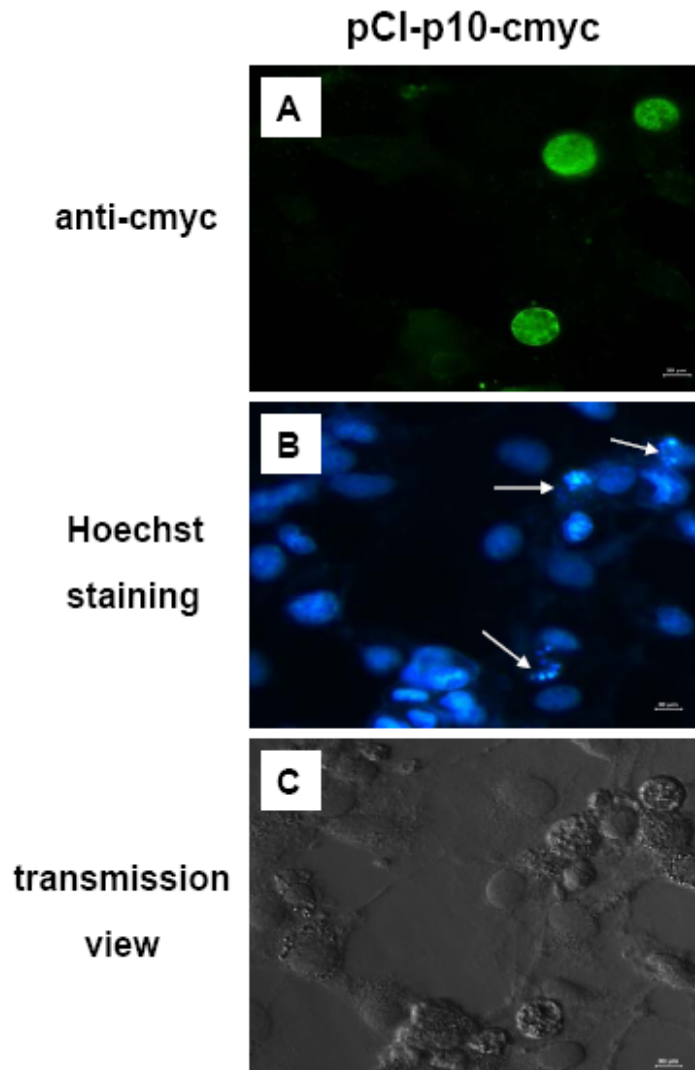
Fig 4.7 The representative fluorescence and transmission photos from the same view showing the abnormal whole cell and nuclei morphology in the p10-cmyc overexpressing Cos-7 cells. (A) Immunocytochemistry of cmyc showing the abnormal morphology of p10-cmyc overexpressing cells. (B) Hoechst staining showing the apoptotic-like pyknosis nuclei in p10-cmyc overexpressing cells. (C) Transmission view.

As cmyc protein did not generate fluorescence by itself, immunocytochemistry was performed according to the protocol described in 2.2.11. Unfortunately, cmyc tag was

too small to retain in the cells after membrane permeation and washing steps in immunocytochemistry process. So it was hard to check morphology of vector expressing cells in fluorescence microscope. Nevertheless, p10-cmyc overexpressing cells were clearly shown in fluorescence microscope after immunocytochemistry and the abnormal whole cell and nuclei morphology were displayed just like those in pEGFP-p10 overexpressing cells. The condensed and fragmented nuclei as indicated by white arrows in Fig 4.7B again suggested that p10-myc expression in Cos-7 cells lead to cell death probably by apoptosis.

4.2.2.3 FACS analysis revealed higher cell death rate in cells subject to pCI-p10-cmyc transfection than those subject to vector control transfection

FACS analysis was performed after the transfection of pCI-p10-myc. As shown in Fig 4.8, Cos-7 cells subject to pCI-p10-myc transfection displayed higher cell death rate than those subject to vector control. This difference was contributed by the small peak in subG1 field as highlighted in the ellipse in Fig4.8B. This suggested the increase of the DNA fragmentation rate among the cells subject to pCI-p10-myc transfection. Values in Fig4.8C are mean±s.d. of three independent experiments. Ten thousand cells were counted for each value. One-side student T test was done and *p<0.05 comparing to vector control.
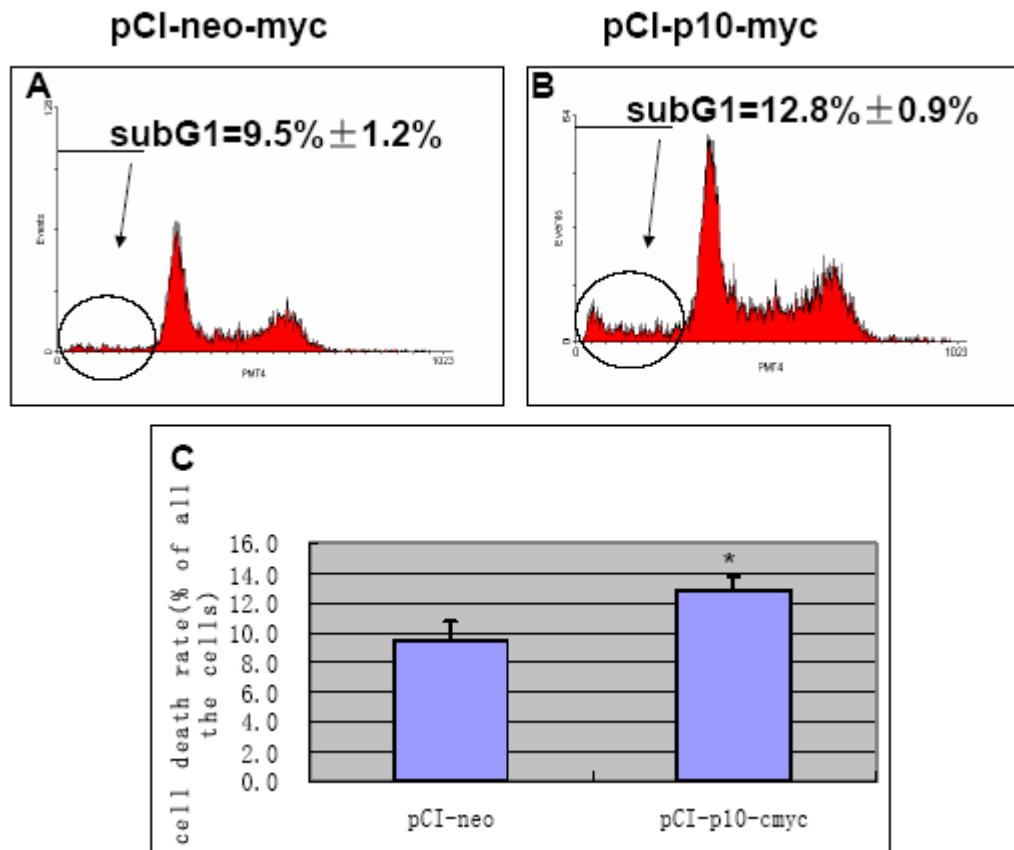
Fig 4.8 Quantification of the cell death rate by FACS analysis. Panel (A) and (B) show the representative FACS pictures of Cos-7 cells subject to pCI-neo-myc and pCI-p10-myc transfection respectively.

4.2.3 Discussion

In this stage, evidence that p10-myc overexpression in Cos-7 cells also mediated cell death were collected. This data confirmed that the toxic effect was caused by p10 and ruled out the two alternative explanations mentioned in 4.1.3. Revealed by fluorescence microscope photos, most of the p10 overexpressing cells displayed cell shrinkage and round shape and some part of them did not show abnormal nuclei. This suggested that the p10 overexpression might be followed by the collapse of the cytoskeleton event

which subsequently triggered some downstream signal pathways and finally led to nuclei degradation. Moreover, as some p10 overexpressing cells displayed membrane blebbing in addition to nuclei fragmentation, both of which are typical apoptosis markers, it is proposed that the p10 overexpressing cells may die by apoptosis.

However, it remained a question whether the toxic effect of p10 was just an accident in Cos-7 cells or not. To answer this question, another cell line called HEK293 would be used for p10 overexpression experiments in the next stage.

4.2.4 Conclusion

Overexpression of p10-cmyc confirmed the toxic effect of p10 in Cos-7. p10 overexpressing caused the disruption of cytoskeleton and possibly induced apoptosis in Cos-7.

4.3 Overexpression of p10-cmyc mediated death of HEK293 cells

4.3.1 Introduction

In the previous work, the evidences were collected to prove that overexpression of p10 mediated Cos-7 cells death. However, Cos-7 cells were from green monkey and they may differ much from human cells. It was necessary to further explore whether the toxic effect of p10 also applied to human cells or was it just an accident in Cos-7 cells. So in this stage, a human cell line HEK293 was subject to transfection experiments and the influence of the p10-myc overexpression was studied. Like Cos-7, HEK293 is also a kidney cell line and often serves as a transfection host. Moreover, the conditions for cell culture and transfection are also similar. After transfection the influence of the p10 overexpression in HEK293 cells would be evaluated by fluorescence microscope and abnormal nuclei assay.

4.3.2 Results

4.3.2.1 48 hours after transfection, p10-cmyc fusion proteins were overexpressed in HEK293 cells

HEK293 were subject to transfection and were harvested 48 hours later. Protein concentrations of the samples were determined by RC DC protein assay kit. 30μg proteins of each sample were loaded into SDS-PAGE gels and the final results were shown in Fig 4.9. Altogether four antibodies were used. In Fig 4.9A, no band was detected in non-transfection Cos-7 samples. The small myc band could not be seen in

vector pCI-neo-myc samples as the reason mentioned previously (refer to 4.2.2.1). The

band of p10-cmyc was clearly shown in pCI-p10-myc samples. This fusion protein

band was confirmed by anti-n20-p35 which recognized the N-terminal portion of p35

(Fig 4.9B). Moreover, an anti-c19-p35 antibody which recognized the C-terminal part

of p35 did not detect any band as expected (Fig 4.9C). Finally, an anti-α-tubulin

antibody was used to confirm that there were about equal amount of protein in each line

(Fig 4.9D).
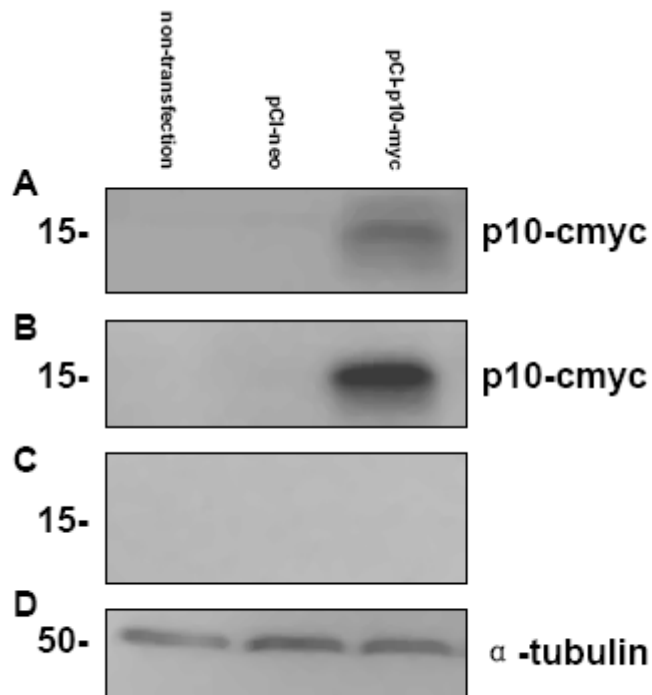
Fig 4.9 Western-blot analysis of the expression of the plasmids in HEK293 cells using

(A) anti-cmyc, (B) anti-n20-p35, (C) anti-c19-p35 and (D) anti- α -tubulin

4.3.2.2 HEK293 overexpressing p10-cmyc also displayed both abnormal whole cell and

nuclei morphology

To detect cmyc positive cells, immunocytochemistry was performed 48 hours after transfection. Like Cos-7, normal HEK293 cells exhibited scattered morphology with prominent lamellipodia. But p10-cmyc overexpressing HEK293 showed cell shrinkage and round cell shape reminiscent of Cos-7 cells overexpressing p10 (Fig 4.10). Moreover, nuclei condensation and fragmentation was detected suggesting apoptosis. This was consistent with the data shown in Fig 4.7 and suggested that the same influence that the overexpression of p10 applied on Cos-7 also applied on HEK293, the human cells.

4.3.2.3 Abnormal nuclei assay revealed high abnormal nuclei rate among HEK293 expressing p10-cmyc

From the data in Table 4.1, it was found that about 35% of the p10-cmyc positive HEK293 cells displayed abnormal nuclei. Actually a large part of the p10-cmyc positive cells only generated weak fluorescence suggesting low level of p10-cmyc and these cells tended to show normal nuclei. Taking this fact into consideration, the abnormal nuclei rate among p10-cmyc overexpressing cells could be higher than 35%. These data again suggested that p10 overexpressing might be quite toxic to HEK293 cells.

	rate1(%)	rate2(%)	rate3(%)	mean(%)	SD(%)
p10-cmyc	34.8	35.7	33.3	34.6	1.2

Table 4.1 The abnormal nuclei rate in p10-cmyc positive HEK293 cells. Data were collected from three independent assays.
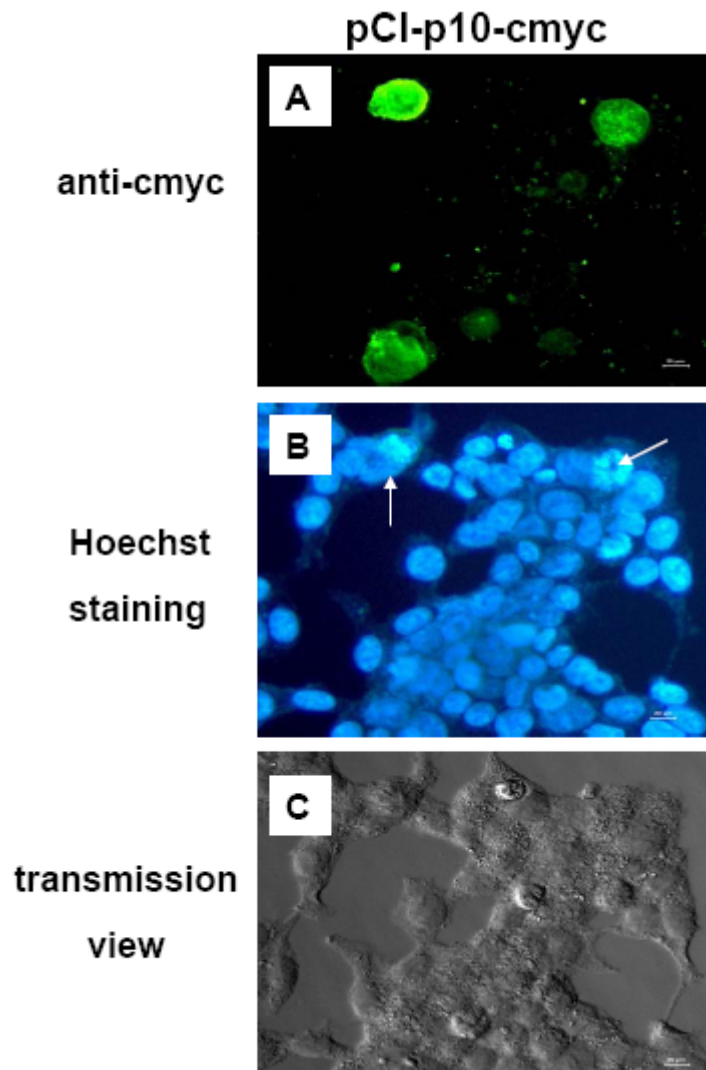
Fig 4.10 The representative fluorescence and transmission photos from the same view showing the abnormal whole cell and nuclei morphology in the p10-cmyc overexpressing HEK293 cells. (A) Immunocytochemistry of cmyc showing the abnormal morphology of p10-cmyc overexpressing cells. (B) Hoechst staining showing the apoptotic-like nuclei in p10-cmyc overexpressing cells. (C) Transmission view.

4.3.3 Discussion

In this stage, overexpression of p10-cmyc in HEK293 cells caused similar toxic effect as observed in Cos-7 cells which suggested that the toxic effect of p10 also applied to human cells. Nevertheless, a weak point of the result was the lack of the data from vector transfected cells. As a matter of fact, cmyc tag itself was only 1.2KD large. It could not be retained on the PVDF membrane for Western-blot detection. In addition, after immunocytochemistry it was often washed away from the cells and making it harder to get a fluorescence photo. That is why the abnormal nuclei assay cannot be performed here. But fortunately the whole cell morphology could be easily observed by transmission view. In vector control well, no obvious cytotoxicity was found. Moreover, no one ever reported that cmyc tag itself could influence the cells and caused any toxic effect. In summary, the results showed that p10 was a toxic protein to HEK293.

However, $p35^{nck5a}$ is a neural-specific protein, so does its derivative p10 which means the kidney cells may never encounter p10 in vivo. So is the toxic effect of p10 to the kidney cells just artificial accident which does not applied to the neuronal cells? To test this possibility, the neuronal cell line should be used in the next stage of the study.

4.3.4 Conclusion

Overexpression of p10-cmyc in HEK293 confirmed that the toxic effect of p10 also applied to human cells.

CHAPTER FIVE

OVEREXPRESSION OF p10 MEDIATES NEURONAL CELL DEATH

5.1 Overexpression of GFP-p10 mediated cell death in neuronal cell line PC12 cells.

5.1.1 Introduction

In the previous chapter, evidence was collected that overexpression of p10 mediated death of mammalian kidney cells. However, $p35^{nck5a}$ is a neural-specific protein and is not endogenously expressed in the kidney cells (Li et al., 2000; Qu et al., 2002). So the kidney cells may never encounter $p35^{nck5a}$ derived p10 protein in vivo which raises the suspicion that the toxic effect of p10 is just an artificial accident. In order to test this possibility, neuronal cell lines were used to collect p10 overexpression data in this chapter.

PC12 cell line is derived from a transplantable rat adrenal pheochromocytoma which responds reversibly to nerve growth factor (Greene *et al.*, 1976). Within several days of exposure to NGF, PC12 cells cease to multiply and begin to extend branching varicose process similar to those produced by sympathetic neurons in primary cell culture. PC12 cells also synthesize and store the catecholamine neurotransmitters dopamine and norepinephrine. Since the generation of PC12 cell line, it has been widely used as a model system for neurobiological and neurochemical studies. It was reported that NGF induced $p35^{nck5a}$ expression in PC12 cells within 24 hours (Harada *et al.*, 2001). Interestingly, PC12 cells are able to express endogenous $p35^{nck5a}$ but before NGF treatment the endogenous $p35^{nck5a}$ are nearly undetectable by immunoblotting. The properties of the PC12 described above make it a good model system for the present

study because the results from PC12 should be more reliable as they are more like neurons than Cos-7 and HEK293 while endogenous $p35^{nck5a}$ in non-differentiated PC12 cells may not largely influence the p10 overexpression results.

5.1.2 Results

5.1.2.1 48 hours after transfection, GFP-p10 fusion proteins were overexpressed in PC12 cells

Altogether four antibodies were used in this experiment. In Fig 5.1A, no band was detected in non-transfection PC12 samples while GFP bands appeared in vector control samples. Meanwhile, both GFP and GFP fusion protein bands appeared in pEGFP-p10 samples. On the other hand, anti-n20-p35 detected a GFP fusion band at the same position as that in Fig 5.1A which confirmed that this band stood for GFP-p10 fusion protein. Moreover, an anti-c19-p35 antibody did not detect any band as expected (Fig 5.1C). Finally, an anti-α-tubulin antibody was used to confirm that there were about equal amount of protein in each line (Fig 5.1D).
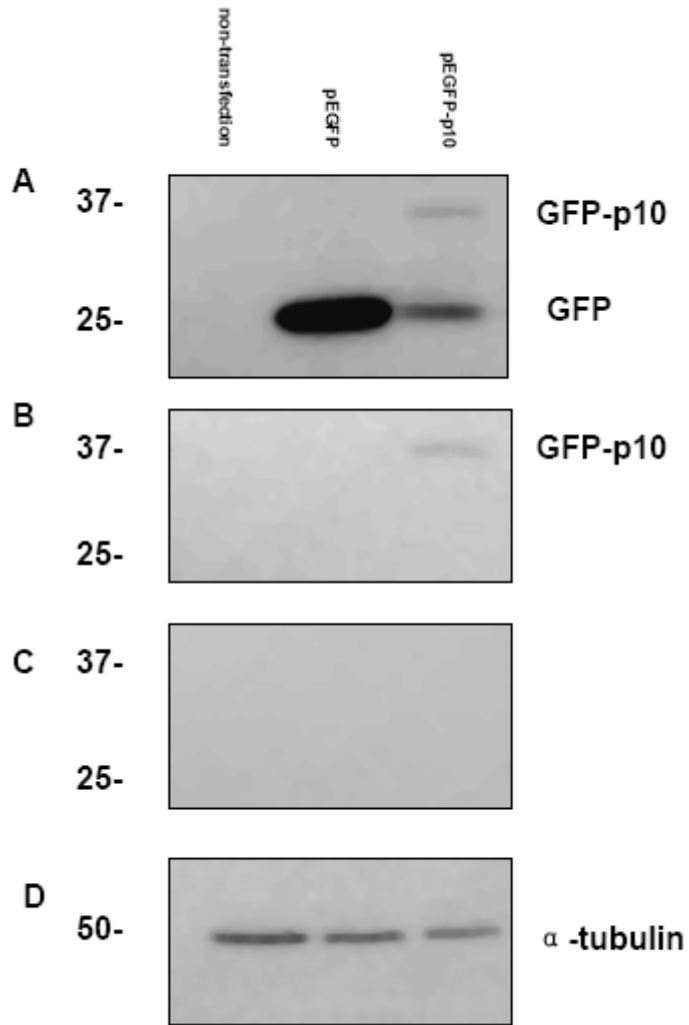
Fig 5.1 Western-blot analysis of the expression of the plasmids in PC12 cells using (A) anti-GFP, (B) anti-n20-p35, (C) anti-c19-p35 and (D) anti- α -tubulin.

5.1.2.2 PC12 overexpressing GFP-p10 also displayed abnormal nuclei
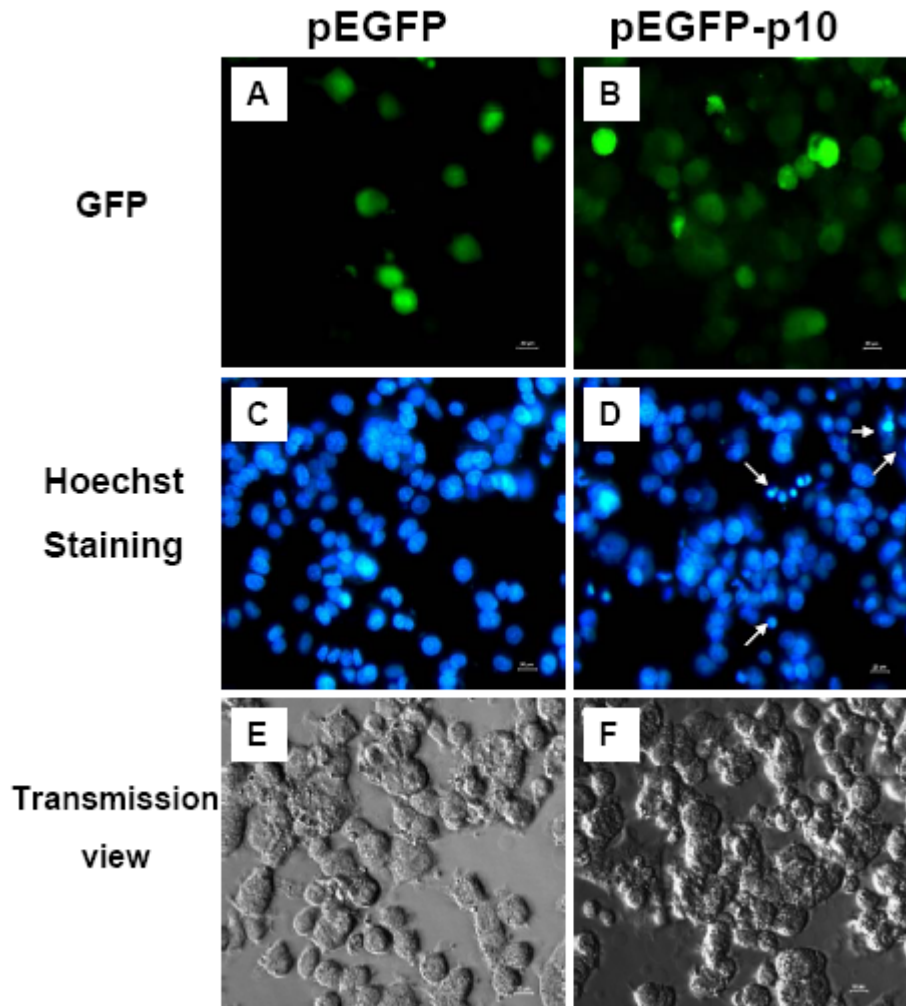
Fig 5.2 The abnormal nuclei of PC12 cells overexpressing GFP-p10 shown by fluorescence photos. Cells transfected with pEGFP-N3 vector control are shown in (A), (C), (E) from the same view while cells transfected with pEGFP-p10 are shown in (B), (D), (F) from the same view. White arrows in (D) indicate the abnormal nuclei which appear condensed or fragmented.

Compared to control cells, some of the GFP-p10 expressing cells displayed condensed or fragmented nuclei as highlighted by the white arrows in Fig 5.2D. Moreover, many cells displayed shrunk round cell bodies as shown in Fig 5.2F which was one of the features of apoptosis.

5.1.3 Discussion

In this stage, GFP-p10 fusion proteins were expressed in non-differentiated neuronal cell line PC12 and pyknosis nuclei were observed. The result suggested that the p10 toxic effect was not limited to kidney cells and also applied to neuronal cell line. The overexpression of GFP-p10 in PC12 seemed to cause the same abnormal nuclei phenomenon as those in Cos-7 and HEK293 (Fig 4.3 and Fig 4.7) which suggested that the overexpression of p10 may trigger the same downstream cell death process. Moreover, this toxic effect may not be just an artificial accident as PC12 cells are capable of expressing endogenous p35^{nck5a} when they are differentiated by NGF.

5.1.4 Conclusion

Overexpression of GFP-p10 in neuronal cell line PC12 led to abnormal nuclei suggesting cell death. This phenomenon was similar to those observed in Cos-7 and HEk293 cells which may indicate that the p10 toxic effect was not an artificial accident and may happen in vivo.

5.2 Overexpression of GFP-p10 interfered with PC12 differentiation

5.2.1 Introduction

In the previous stage, overexpression of GFP-p10 in non-differentiated PC12 cells was proved to cause abnormal nuclei and probably lead to cell death. As mentioned before, non-differentiated PC12 cells respond to NGF and differentiate to neuron-like cells. On differentiation, they express some neuro-specifc proteins such as $p35^{nck5a}$ which subsequently activate Cdk5. The differentiation process may trigger and activate a neuro-specifc protein network. The study of the p10 overexpression on the PC12 differentiation may give more information on the p10 influence of the neuronal cells.

5.2.2 Results

5.2.2.1 PC12 was differentiated to neuron-like cells by NGF

In Fig 5.3 A, C ,E, non-differentiated PC12 cells generally showed cell bodies with very short or nearly no axon projection. The morphology of the non-differentiated PC12 cells did not change from day 1 to day 3. On the other hand, differentiated PC12 cells displayed obvious axon projection since day 1 as shown in Fig 5.3 B, D, F. As time went by, the axon shafts grew longer and longer and tended to form a complex network among each other similar to the neuron network. Moreover, most of the differentiated PC12 cells ceased to divide as the confluence of the cells from day 1 to day 3 did not increase much while non-differentiated PC12 cells multiplied much faster.

non-differentiated   differentiated

day 1

day 2

day 3
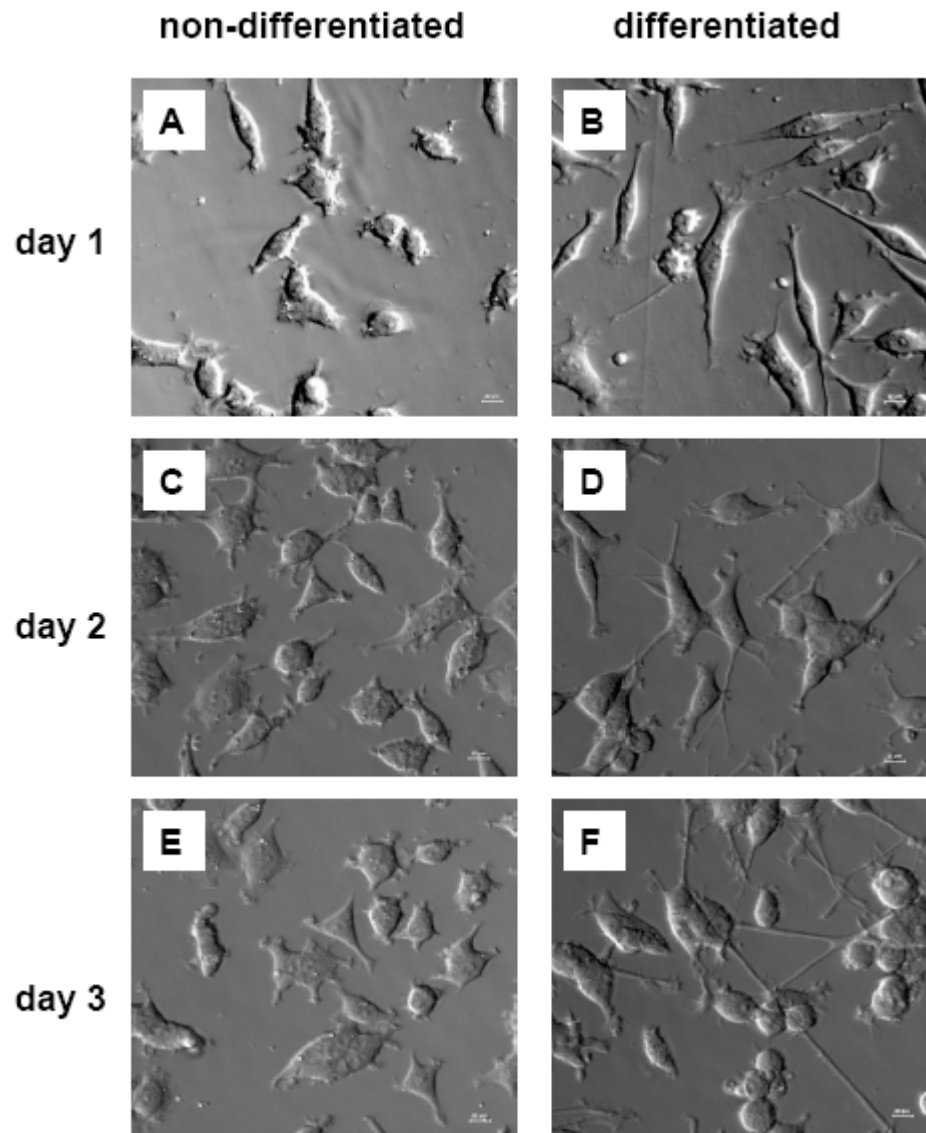
Fig 5.3 Differentiated PC12 cells were cultured in complete growth medium with 100ng/ml NGF while non-differentiated PC12 cells were cultured in complete growth medium only. Non-differentiated PC12 from day 1 (day 1 means 1 day after treatment) to day 3 were shown in A, C, E and differentiated PC12 in B, D, F.

5.2.2.2 NGF treatment induced PC12 to express p35^{nck5a}

Western-blot analysis showed that non-differentiated PC12 cells expressed no detectable p35^{nck5a} while endogenous p35^{nck5a} appeared on the membrane since 1 day after NGF treatment (Fig 5.4 A). Anti-β-actin was used as internal control (Fig 5.4 B).
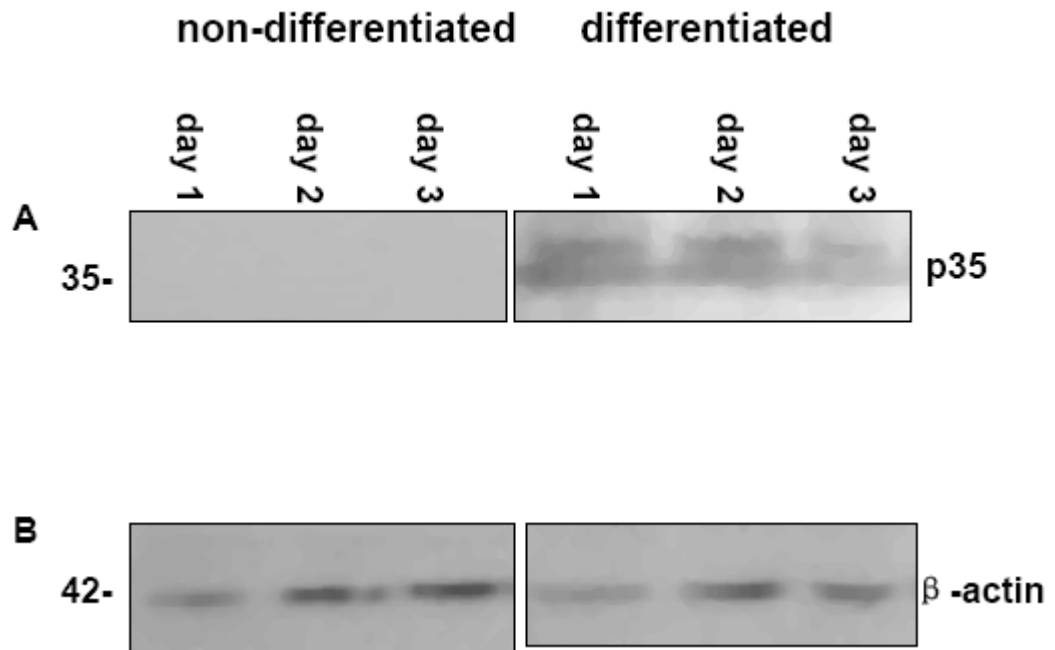
Fig 5.4 Western-blot analysis of p35^{nck5a} expression in PC12 cells using (A) anti-c19-p35 and (B) anti-β-actin.

5.2.2.3 PC12 differentiation process was interfered by GFP-p10 overexpression

Cells were subject to transfection for about 24 hours. Then differentiation reagent was added. Another 24 hours later, photos were taken. Axon projection appeared normal in vector samples suggesting GFP alone did not influence PC12 differentiation much (Fig 5.5 A, C). However, most of the GFP-p10 expressing cells did not respond to NGF well. Instead of extending axon branches from the cell body, cells tended to shrink and aggregate to form clumps.
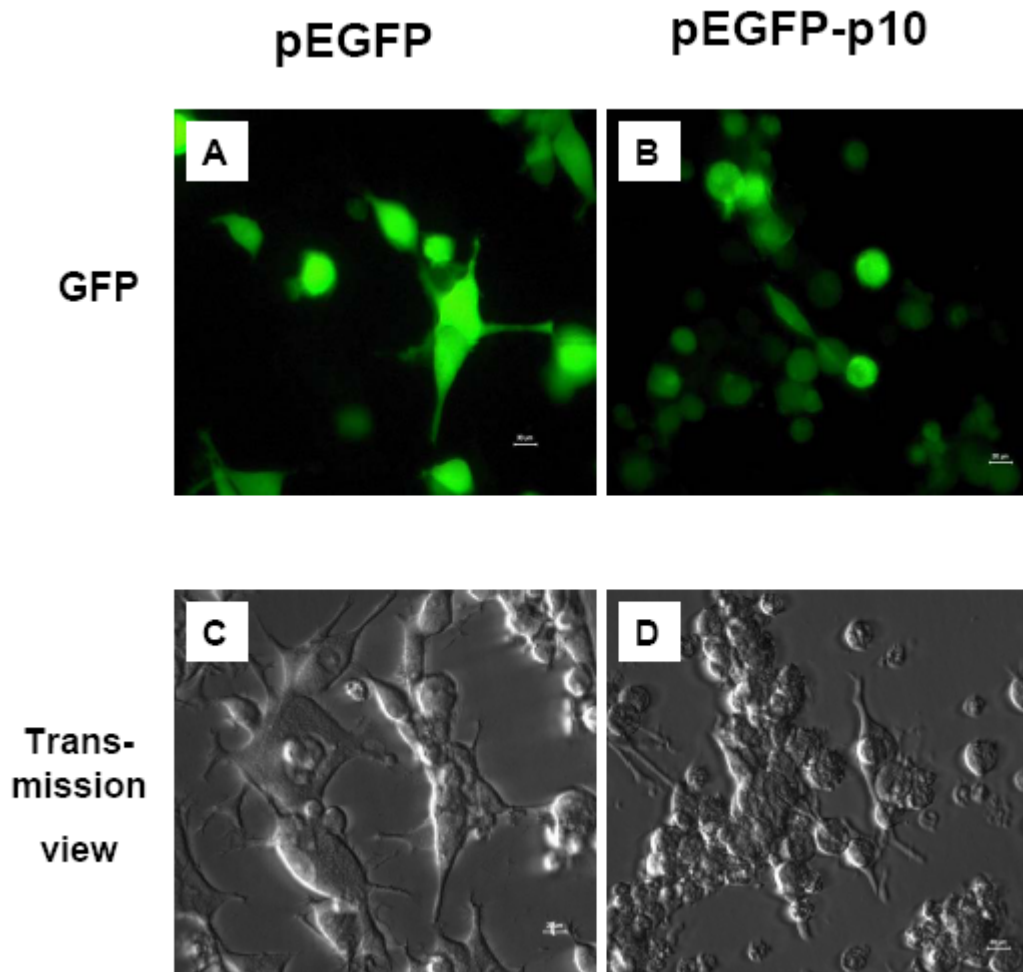
Fig 5.5 The whole cell morphology shown by fluorescence and transmission photos. Vector transfected cells were shown in fluorescence photo (A) and transmission photo (C) from the same view. pEGFP-p10 transfected cells were shown in fluorescence photo (B) and transmission photo (D) from the same view.

5.2.3 Discussion

In this stage, PC12 cells were subject to NGF differentiation after transfection and the results showed that GFP-p10 overexpression might interfere with the PC12 differentiation process. There may be two reasons for this GFP-p10 interference

phenomenon. First, the cells did not respond to NGF differentiation because they had already initiated a death process such as apoptosis that interfered with the differentiation process. Second, the cytoskeleton systems had collapsed as suggested by the shrinking round cell morphology. The collapse of the cytoskeleton systems made the axon projection impossible.

So far following p10 overexpression, two major phenomena had been observed, shrinking round cell morphology and abnormal pyknosis nuclei. However, the two phenomena seemed not to happen at the same time because a large part of the cells with abnormal whole cell morphology did not show abnormal nuclei. It was assumed that the whole cell morphology changed before nuclei morphology, which means that the collapse of the cytoskeleton systems was probably an earlier event than abnormal nuclei. Moreover, it was possible that the former induced the latter.

5.2.4 Conclusion

NGF induced PC12 differentiation to neuron-like cells and the overexpression of GFP-p10 might interfered with this differentiation process probably by causing the collapse of the cytoskeleton systems.

5.3 Caspase-3 was not cleaved in pEGFP-p10 overexpressed Neuro-2a cells

5.3.1 Introduction

In the previous section, pEGFP-p10 was overexpressed in a neuronal cell line, PC12 and seemed to induce cell injury. The pyknosis nuclei suggested that apoptosis might

be involved in this cell injury phenomenon. There is a diversity of groups of molecules involved in the apoptosis pathway. One set of mediators implicated in apoptosis comes from the aspirate-specific cysteinyl protease family called caspases. Among the family members, caspases-3 is considered as a key mediator of apoptosis of mammalian cells. Original caspase-3 exists in the cells as an inactive proenzyme. On initiation of the apoptosis, other enzymes may cleave caspases-3 and turn it into a smaller protein, which is active caspases-3. As there was no good antibody available for detecting active caspase-3 in PC12 cells, I used neuro-2a cells instead for western blot analysis to check whether caspase-3 was activated after p10 overexpression.

5.3.2 Results and discussion
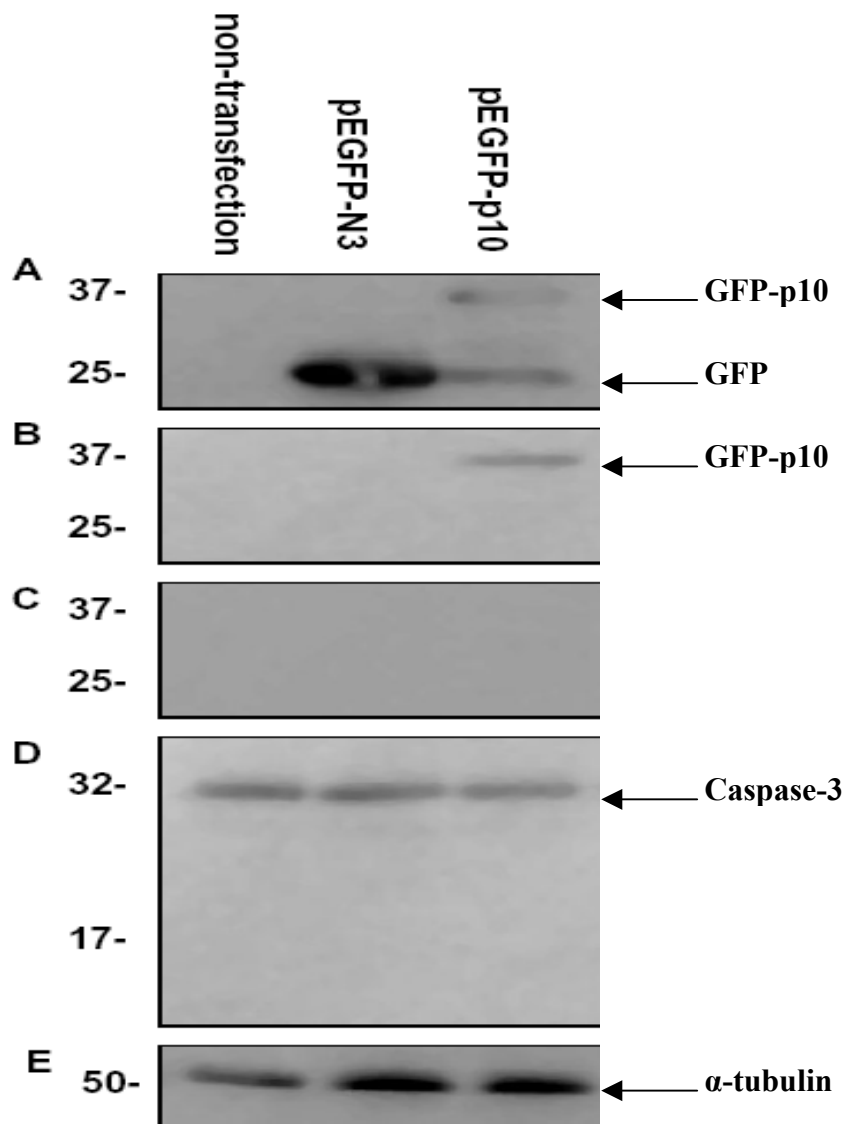
Fig 5.6 Western-blot analysis of the expression of the plasmids and the indigenous Caspase-3 in Neuro-2a cells using (A) anti-GFP, (B) anti-n20-p35, (C) anti-c19-p35, (D) anti-caspase-3, and (E) anti-α-tubulin.

Original caspase-3 is a 32KD proenzyme. On activation, caspase-3 can be cleaved and release a 17KD fragment. Fig 5.6 showed that no 17KD fragment of Caspase-3 was detected after the overexpression of pEGFP-p10 in the Neuro-2a cells. The indigenous caspase-3 levels remained unchanged although through fluorescence microscope (data not shown) it was found that Neuro-2a cells overexpressing pEGFP-p10 displayed the same abnormal whole cell morphology as PC12 cells. The result suggested that the overexpression of p10 might cause cell injury in a caspase-3 independent manner.

5.3.3 Conclusion

Indigenous caspase-3 was not cleaved in pEGFP-p10 overexpressing Neuro-2a cells which suggested that the cell injury mediated by p10 may be caspase-3 independent.

CHAPTER SIX

GENERAL DISSCUSION AND FUTURE WORK

6.1 General discussion

One of the major features of Alzheimer's disease (AD) is the progressive cell loss in several areas of the brain. An understanding of the molecular mechanism of the abnormal neuronal cell death will provide invaluable insights into the cause of the disease and may even help to find the cure of the disease. Moreover, as all other neurodegenerative diseases such as Parkinson's disease, Huntington's disease, and Amyotrophic Lateral Sclerosis are marked by the loss of nerve cells, the study of neuronal cell death in AD may benefit the research of the other neurodegenerative diseases. Therefore, the present study sought to explore the influence of the overexpression of p10, a truncated form of p35^{nck5a} which is possibly implicated in neuronal cell death in AD, on different mammalian cells including neuronal cell lines.

The Cdk5/p35 pathway is recently a hot research topic in terms of the molecular mechanism of AD for the complex is a major candidate responsible for the hyperphosphorylation of tau proteins which ultimately form neurofibrillary tangles, the hallmark of AD. Under such neurotoxic conditions as in AD brains the protease calpain is abnormally activated and mediates the cleavage of p35 to p25 (Lee *et al.*, 2000). Many scientists believe that the association of p25 with Cdk5 causes the abnormal activation of Cdk5 and leads to tau hyperphosphorylation (Patrick *et al.*, 1999; Ahlijianian *et al.*, 2002). However, conflicting evidences were accumulated against the p25 theory (Takashima *et al.*, 2001; Kerokoski *et al.*, 2002; Tandon *et al.*, 2003). Moreover, it is still not clear about the relationship between tau hyperphosphorylation and neuronal cell death.

In Chapter 4, it was shown that overexpression of p10 mediated cell death in kidney cell lines. This is an interesting new finding as no report exists to relate p10 to cell death. Notably, p10 is a product of the cleavage of p35 by calpain under certain neurotoxic conditions. It was previously thought to be membrane-bound and confine p35 to certain compartment of the cells before cleavage because p10 contained a conserved myristoylation sequence (Patrick *et al.*, 1999). But the fate of p10 after p35 cleavage has not been studied. It is possible that p10 is proteolysed and cleared by proteasomes since they are also responsible for the clearance of p35 (Patrick *et al.*, 1998). Moreover, it was reported that proteasome functions were impaired in AD brains (Keller *et al.*, 2000). Therefore, p10 may be accumulated in AD brains for at least two reasons. On one hand, calpain is abnormally activated (Saito *et al.*, 1993) and produces more p10 proteins than normal. On the other hand, proteasome activity is decreased and leaves more p10 proteins uncleared.

More interestingly, it was reported that there was no detectable Cdk5 expression in Cos-7 (Qu *et al.*, 2002) and barely detectable Cdk5 expression in HEK293 (Li *et al.*, 2000). This means that p10 is capable of mediating cell death independent of Cdk5 activity. Actually, Cdk5 activity is intensively regulated in terms of the life or death choice (Shelton and Johnson, 2004). Sometimes Cdk5 showed pro-apoptotic functions (Patrick *et al.*, 1999; Zhang and Johnson, 2000; Weishaup *et al.*, 2003; Zhang *et al.*, 2002) but sometimes it displayed anti-apoptotic functions (Li *et al.*, 2003; Li *et al.*, 2002; Kerokoski *et al.*, 2001). So it seems that Cdk5 and its many downstream substrates interplay in a convoluted network to keep balance between life and death. A

huge force may be required to drive the whole network out of the track and sliding down to death which seems not possible. On the other side, p10 is not a kinase, as far as we know, and may not be subject to intensive regulation in vivo which gives it more of a chance to accumulate in vivo. Therefore, it is conceivable that the cleavage of p35 frees p10 besides p25 to initiate its toxic effect on the cells and the accumulation of p10 may contribute to neuronal cell death in AD brains.

If p10 has toxic effect, how is it brought about? Here I propose that the key may lie in the myristoylation signal at the N-terminal of the protein p10. The myristoylation is a post-transcriptional modification mediated by the cytosolic enzyme, N-myristoyltransferase (Boutin, 1997). This sort of modification is absolutely specific to the N-terminal amino acid glycine in proteins. Previous studies have shown that myristoylation not only greatly favors the association of the protein to a membrane, but also makes the protein in close contact with its substrates, cofactors, and "receptors" which subsequently drives the cellular signaling chain forward. Interestingly, one study suggested that certain myristoylation may activate an additional death signaling pathway (Kim *et al.*, 1995). Moreover, a Glycine to Alanine mutation at the N-terminal of p35 which abolishes the myristoylation signal reduced the rate of fragmented nuclei in neurons from 20% to about 10% which implied the involvement of myristoylation signal in neuronal cell death (Patrick *et al.*, 1999). Therefore, it is possible that the cleavage of p35 produces free p10 which subsequently initiates a death signaling pathway and finally leads to cell death.

6.2 Future work

The present study reveals the toxic effect of p10 overexpression in mammalian cells and opens a new research topic in terms of the molecular mechanism of neuronal cell death in Alzheimer's disease. To make the p10 story clearer, some of the following work is listed below. First, it is worthwhile to compare the p10 level in Alzheimer's brains with control brains and see whether p10 proteins are accumulated in Alzheimer's brains because the result may directly link p10 story to Alzheimer's disease. Second, the effect of p10 overexpression in primary neurons needs to be explored in the future. Although lipofection efficiency of primary neurons is quite low, application of a newly developed and commercially available product called Nupherin-neuron may solve this problem (Subramanian *et al.*, 1999). The absence of nuclear envelope breakdown and the low probability of transport across the nuclear pore complex in nondividing cells like primary neurons are major obstacles to efficient lipofection. Nupherin-neuron consists of a cationic peptide fused to a nonclassical nuclear localization sequence which helps to target the lipid-DNA complex to nuclei and facilitates the entry of the complex into the nuclei. And it was reported that the application of Nupherin-neuron together with lipofectant increased the lipofection efficiency of rat hippocampal neurons from less than 0.5% to more than 20% (Ma *et al.*, 2002). Therefore, the high lipofection efficiency of non-dividing cells achieved by Nupherin-neuron paves the way for p10 overexpression experiments in primary neurons. Finally, the generation of a G2A mutation which abolishes myristoylation on the p10 protein may provide a good

research tool for further research of the function of myristoylation signal on p10 and its relationship to cell death.

Bibliography

Ahlijanian, M.K., Barrezueta, N.X., Williams, R.D., Jakowski, A., Kowsz, K.P., McCarthy S., Coskran, T., Carlo, A., Seymour, P.A., Burkhardt, J.E., Nelson, R.B., McNeish, J.D. (2000). Hyperphosphorylated tau and neurofilament and cytoskeletal disruptions in mice expressing human p25, an activator of Cdk5. *P. Natl. Acad. Sci. USA*, 97(6), 2910-1915.

Arioka, M., Tsukamoto, M., Ishiguro, K., Kato, R., Sato, K., Imahori, K., Uchida, T. (1993). Tau protein kinase II is involved in the regulation of the normal phosphorylation state of tau protein. *J. Neurochem.*, 60(2), 461-468.

Blechman, E.A., Brownell, K.D. (1998). *Behavioral medicine and women: a comprehensive handbook*. New York: Guilford Press.

Boutin, J.A. (1997). Myristoylation. *Cell Signal.*, 9(1), 15-35.

Chae, T., Kwon, Y.T., Bronson, R., Dikkes, P., Li, E., Tsai, L.H. (1997). Mice lacking p35, a neuronal specific activator of Cdk5, display cortical lamination defects, seizures, and adult lethality. *Neuron*, 18(1), 29-42.

Chen, M., Fernandez, H.L. (2001). Where do Alzheimer's plaques and tangles come from? Aging-induced protein degradation inefficiency. *Front Biosci.*, 6, E1-E11.

Dhavan, R., Tsai, L.H. (2001). A decade of Cdk5. *Nat. Rev. Mol. Cell Biol.*, 2(10), 749-759.

Elledge, S.J., Spottswood, M.R. (1991). A new human p34 protein kinase, CDK2, identified by complementation of a cdc28 mutation in Saccharomyces cerevisiae, is a homolog of Xenopus Eg1. *EMBO J.*, 10(9), 2653-2659.

Greene, L.A., Tischler, A.S. (1976). Establishment of a noradrenergic clonal line of rat adrenal pheochromocytoma cells which respond to nerve growth factor. *P. Natl. Acad. Sci. USA*, 73(7), 2424-2428.

Harada, T., Morooka, T., Ogawa, S., Nishida, E. (2001). ERK induces p35, a neuron-specific activator of Cdk5, through induction of Egr1. *Nat. Cell Biol.*, 3(5), 453-459.

Harwood, D.G., Barker, W.W., Ownby, R.L., Mullan, M., Duara, R. (2002). Apolipoprotein E polymorphism and cognitive impairment in a bi-ethnic community-dwelling elderly sample. *Alzheimer Dis. Assoc. Disord.* 16(1), 8-14.

Hook, V.Y., Sei, C., Yasothornsrikul, S., Toneff, T., Kang, Y.H., Efthimiopoulos, S., Robakis, N.K., Van Nostrand, W. (1999). The kunitz protease inhibitor form of the amyloid precursor protein (KPI/APP) inhibits the proneuropeptide processing enzyme prohormone thiol protease (PTP). Colocalization of KPI/APP and PTP in secretory vesicles. *J. Biol. Chem.*, 274(5), 3165-3172.

Humbert, S., Dhavan, R., Tsai, L.H. (2000a). p39 activates Cdk5 in neurons, and is associated with the actin cytoskeleton. *J. Cell Sci.*, 113, 975-983.

Humbert, S., Lanier, L.M., Tsai, L.H. (2000b). Synaptic localization of p39, a neuronal activator of Cdk5. *Neuroreport*, 11(10), 2213-2216.

Ihara, Y., Nukina, N., Miura, R., Ogawara, M. (1986). Phosphorylated tau protein is integrated into paired helical filaments in Alzheimer's disease. *J. Biochem.*, 99(6), 1807-1810.

Imahori, K., Uchida, T. (1997). Physiology and pathology of tau protein kinases in relation to Alzheimer's disease. *J. Biochem.*, 121(2), 179-188.

Ishiguro, K., Takamatsu, M., Tomizawa, K., Omori, A., Takahashi, M., Arioka, M., Uchida, T. (1992). Tau protein kinase I converts normal tau protein into A68-like component of paired helical filaments. *J. Biol. Chem.*, 267(15), 10897-10901.

Kang, J., Lemaire, H.G., Unterbeck, A., Salbaum, J.M., Masters, C.L., Grzeschik, K.H., Multhaup, G., Beyreuther, K., Muller-Hill, B. (1987). The precursor of Alzheimer's disease amyloid A4 protein resembles a cell-surface receptor. *Nature*, 325(6106), 733-736.

Keller, J.N., Hanni, K.B., Markesbery, W.R. (2000). Impaired proteasome function in Alzheimer's disease. *J. Neurochem.*, 75(1), 436-439.

Kerokoski, P., Suuronen, T., Salminen, A., Soininen, H., Pirttila, T. (2002). Cleavage of the cyclin-dependent kinase 5 activator p35 to p25 does not induce tau hyperphosphorylation. *Biochem. Biophys. Res. Commun.*, 298(5), 693-698.

Kerokoski, P., Suuronen, T., Salminen, A., Soininen, H., Pirttila, T. (2001). The levels of Cdk5 and p35 proteins and tau phosphorylation are reduced during neuronal apoptosis. *Biochem. Biophys. Res. Commun.*, 280(4), 998-1002.

Kesavapany, S., Lau, K.F., Mcloughlin, D.M., Brownlees, J., Ackerley, S., Leigh, P.N., Shaw, C.E., Miller, C.C. (2001). p35/Cdk5 binds and phosphorylates beta-catenin and regulates beta-catenin/presenilin-1 interaction. *Eur. J. Neurosci.*, 13(2), 241-247.

Kim, C.H., Song, Y.H., Park, K., Oh, Y., Lee, T.H. (1995). Induction of cell death by myristylated death domain of p55 TNF receptor is not abolished by Iprcg-like point mutation in death domain. *J. Inflamm.*, 45(4), 312-322.

Kitaguchi, N., Takahashi, Y., Tokushima, Y., Shiojiri, S., Ito, H. (1988). Novel precursor of Alzheimer's disease amyloid protein shows protease inhibitory activity. *Nature*, 331(6156), 530-532.

Kwon, Y.T., Tsai, L.H., Crandall, J.E. (1999). Callosal axon guidance defects in p35 (-/-) mice. *J. Comp. Neurol.*, 415(2), 218-229.

Lee, K.Y., Rosales, J.L., Tang, D., Wang, J.H. (1996). Interaction of cyclin-dependent kinase 5 (Cdk5) and neuronal Cdk5 activator in bovine brain. *J. Biol. Chem.*, 271(3), 1538-1543.

Lew, J., Qi, Z., Huang, Q.Q., Paudel, H., Matsuura, M., Zhu, X., Wang, J.H. (1995). Structure, function, and regulation of neuronal Cdc2-like protein kinase. *Neurobiol. Aging*, 16(3), 263-268.

Li, B.S., Zhang, L., Takahashi, S., Ma, W., Jaffe, H., Kulkarni, A.B., Pant, H.C. (2002). Cyclin-dependent kinase 5 prevents neuronal apoptosis by negative regulation of c-Jun N-terminal kinase 3. *EMBO J.*, 21(3), 324-333.

Li, B.S., Zhang, L., Gu, J., Amin, N.D., Pant, H.C. (2000). Integrin α1β1-mediated activation of cyclin-dependent kinase 5 activity is involved in neurite outgrowth and human neurofilament protein H Lys-Ser-Pro tail domain phosphorylation. *J. Neurosci.*, 20(16), 6055-6062.

Li, G., Faibushevich, A., Turunen, B.J., Yoon, S.O., Georg, G., Michaelis, M.L., Dobrowsky, R.T. (2003). Stabilization of the cyclin-dependent kinase 5 activator, p35, by paclitaxel decreases beta-amyloid toxicity in cortical neurons. *J. Neurochem.*, 84(2), 347-362.

Liu, F., Su, Y., Li, B., Zhou, Y., Ryder, J., Gonzelez-DeWhitt, P., May, P.C., Ni, B. (2003). Regulation of amyloid precursor protein (APP) phosphorylation and processing by p35/Cdk5 and p25/Cdk5. *FEBS Lett.*, 547(1-3), 193-196.

Lodish, H., Berk, A., Zipursky, S.L., Matsudaira, P., Baltimore, D., Darnell, J.E. (2000). *Molecular Cell Biology*, fourth edition. New York: W.H. Freeman & Company.

Ma, H., Zhu, J., Maronski, M., Kotzbauer, P.T., Lee, V.M., Dichter, M.A., Diamond, S.L. (2002). Non-classical nuclear localization signal peptides for high efficiency lipofection of primary neurons and neuronal cell lines. *Neuroscience*, 112(1), 1-5.

Maccioni, R.B., Munoz, J.P., Barbeito, L. (2001). The molecular bases of Alzheimer's disease and other neurodegenerative disorders. *Arch. Med. Res.*, 32(5), 367-381.

Meyerson, M., Enders, G.H., Wu, C.L., Su, L.K., Gorka, C., Nelson, C., Harlow, E., Tsai, L.H. (1992). A family of human cdc2-related protein kinases. *EMBO J.*, 11(8), 2909-2917.

Nikolic, M., Dudek, H., Kwon, Y.T., Ramos, Y.F., Tsai, L.H. (1996). The Cdk5/p35 kinase is essential for neurite outgrowth during neuronal differentiation. *Genes Dev.*, 10(7), 816-825.

Ohshima, T., Gilmore, E.C., Longenecker, G., Jacobowitz, D.M., Brady, R.O., Herrup, K., Kulkarni, A.B. (1999). Migration defects of Cdk5 (-/-) neurons in the developing cerebellum is cell autonomous. *J. Neurosci.*, 19(14), 6017-6026.

Ohshima, T., Ward, J.M., Huh, C.G., Longenecker, G., Veeranna, Pant, H.C., Brady, R.O., Martin, L.J., Kulkarni, A.B. (1996). Targeted disruption of the cyclin-dependent kinase 5 gene results in abnormal corticogenesis, neuronal pathology and perinatal death. *P. Natl. Acad. Sci. USA*, 93(20), 11173-11178.

Paglini, G., Peris, L., Diez-Guerra, J., Quiroga, S., Caceres, A. (2001). The Cdk5-p35 kinase associates with the Golgi apparatus and regulates membrane traffic. *EMBO Rep.*, 2(12), 1139-1144.

Parnavelas, J.G. (2000). The origin and migration of cortical neurons: new vistas. *Trends Neuronsci.*, 23(3), 126-131.

Patrick, G.N., Zhou, P., Kwon, Y.T., Howley, P.M., Tsai, L.H. (1998). p35, the neuronal-specific activator of cyclin-dependent kinase 5 (Cdk5) is degraded by the ubiquitin-proteasome pathway. *J. Biol. Chem.*, 273(37), 24057-24064.

Patrick, G.N., Zukerberg, L., Nikolic, M., de la Monte, S., Dikkes, P., Tsai, L.H. (1999). Conversion of p35 to p25 deregulates Cdk5 activity and promotes neurodegeneration. *Nature*, 402(6762), 615-622.

Pike, C.J., Overman, M.J., Cotman, C.W. (1995). Amino-terminal deletions enhance aggregation of beta-amyloid peptides in vitro. *J. Biol. Chem.*, 270(41), 23895-23898.

Qu, D., Li, Q., Lim, H.Y., Cheung, N.S., Li, R., Wang, J.H., Qi, R.Z. (2002). The protein SET binds the neuronal Cdk5 activator p35nck5a and modulates Cdk5/p35nck5a activity. *J. Biol. Chem.*, 277(9), 7324-7332.

Rapoport, M., Dawson, H.N., Binder, L.I., Vitek, M.P., Ferreira, A. (2002). Tau is essential to beta-amyloid-induced neurotoxicity. *P. Natl. Acad. Sci. USA*, 99(9), 6364-6369.

Saito, K. Elce, J.S., Hamos, J.E., Nixon,R.A. (1993). Widespread activation of calcium-activated neutral protease (calpain) in the brain in Alzheimer disease: a potential molecular bases for neuronal degradation. *P. Natl. Acad. Sci. USA*, 90(7), 2628-2632.

Shelton, S.B., Johnson, G.V. (2004). Cyclin-dependent kinase-5 in neurodegeneration. *J. Neurochem.*, 88(6), 1313-1326.

Smith, D.S., Greer, P.L., Tsai, L.H. (2001). Cdk5 on the brain. *Cell Growth Differ.*, 12(6), 277-283.

Subramanian, A., Ranganathan, P., Diamond, S.L. (1999). Nuclear targeting peptide scaffolds for lipofection of nondividing mammalian cells. *Nat. Biotechnol.*, 17(9), 873-877.

Takashima, A., Murayama, M., Yasutake, K., Takahashi, H., Yokoyama, M., Ishiguro, K. (2001). Involvement of cyclin dependent kinase5 activator p25 on tau phosphorylation in mouse brain. *Neurosci. Lett.*, 306(1-2), 37-40.

Tandon, A., Yu, H., Wang, L., Rogaeva, E., Sato, C., Chishti, M.A., Kawarai, T., Hasegawa, H., Chen, F., Davies, P., Fraser, P.E., Westaway, D., St George-Hyslop, P.H. (2003). Brain levels of CDK5 activator p25 are not increased in Alzheimer's or other neurodegenerative diseases with neurofibrillary tangles. *J. Neurochem.*, 86(3), 572-581.

Tang, D., Yeung, J., Lee, K.Y., Matsushita, M., Matsui, H., Tomizawa, K., Hatase, O., Wang, J.H. (1995). An isoform of the neuronal cyclin-dependent kinase 5 (Cdk5) activator. *J. Biol. Chem.*, 270(45), 26897-26903.

Taniguchi, S., Fujita, Y., Hayashi, S., Kakita, A., Takahashi, H., Murayama, S., Saido, T.C., Hisanaga, S., Iwatsubo, T., Hasegawa, M. (2001). Calpain-mediated degradation of p35 to p25 in postmortem human and rat brains. *FEBS Lett.*, 489(1), 46-50.

Terpe, K. (2003). Overview of tag protein fusions: from molecular and biochemical fundamentals to commercial systems. *Appl. Microbiol. Biotechnol.*, 60(5), 523-533.

Terry, R.D., Katzman, R., Bick, K.L. (1994). *Alzheimer disease*. New York: Raven Press.

Tsai, L.H., Delalle, I., Caviness, V.S. Jr, Chae, T., Harlow, E. (1994). p35 is a neural-specific regulatory subunit of cyclin-dependent kinase 5. *Nature*, 371(6496), 419-423.

Tseng, H.C., Zhou, Y., Shen, Y., Tsai, L.H. (2002). A survey of Cdk5 activator p35 and p25 levels in Alzheimer's disease brains. *FEBS Lett.*, 523(1-3), 58-62.

Vila, M., Przedborski, S. (2003). Targeting programmed cell death in neurodegenerative diseases. *Nat. Rev. Neurosci.*, 4(5), 365-375.

Washbourne, P., McAllister, A.K. (2002). Techniques for gene transfer into neurons. *Curr. Opin. Neurobiol.*, 12(5), 566-573.

Weishaupt, J.H., Kussmaul, L., Grotsch, P., Heckel, A., Rohde, G., Romig, H., Bahr, M., Gillardon, F. (2003). Inhibition of CDK5 is protective in necrotic and apoptotic paradigms of neuronal cell death and prevents mitochondrial dysfunction. *Mol. Cell Neurosci.*, 24(2), 489-502.

Whitehouse, P.J., Maurer, K., Ballenger, J.F. (2000). *Concepts of Alzheimer disease: biological, clinical, and cultural perspectives.* Chapter one. Baltimore: Johns Hopkins University Press.

Yoo, B.C., Lubec, G. (2001). p25 protein in neurodegeneration. *Nature*, 411(6839), 763-764.

Zhang, J., Johnson, G.V. (2000). Tau protein is hyperphosphorylated in a site-specific manner in apoptotic neuronal PC12 cells. *J. Neurochem.*, 75(6), 2346-2357.

Zhang, J., Krishnamurthy, P.K., Johnson, G.V. (2002). Cdk5 phosphorylates p53 and regulates its activity. *J. Neurochem.*, 81(2), 307-313.

Zhang, Z., Hartmann, H., Do, V.M., Abramowski, D., Sturchler-Pierrat, C., Staufenbiel, M., Sommer, B., van de Wetering, M., Clevers, H., Saftig, P., De Strooper, B., He, X., Yankner, B.A. (1998). Destabilization of beta-catenin by mutations in presenilin-1 potentiates neuronal apoptosis. *Nature*, 395(6703), 698-702.

Appendix A: Culture Media

1. Cell culture media and serum (all sterilized):

DMEM (Sigma, D1152)

Fetal Bovine Serum (Hyclone, ch30160.03)

Horse Serum (Sigma, H1270)

2. Bacterial media:

LB broth: LB powder (Sigma, L3152) dissolve in Milli-Q water (25g/L), autoclave at

121˚C for 20 min.

Agarose for LB broth: Agar Granulated (DIFCO, 214530), supply as 1% (w/v) in LB.

3. E.coli strain:

strain name: DH5 α

strain genotype: SupE44 placU169 (φ80lacZρM115) hsdR17 recA1 endA1 gyrA96

thi-1 relA1

Appendix B: Plasmids

1. pEGFP-N3 vector (BD Clontech, 6080-1):

pEGFP-N3 Vector Information
GenBank Accession #: U57609

PT3054-5
Catalog #6080-1

```
591        601        611        621        631        641        651        661        671           EGFP
 .          .          .          .          .          .          .          .          .           ──────▶
GCT AGC GCT ACC GGA CTC AGA TCT CGA GCT CAA GCT TCG AAT TCT GCA GTC GAC GGT ACC GCG GGC CCG GGA TCC ATC GCC ACC ATG GTG
Nhe I Eco47 III      Bgl II  Xho I \   Hind III  EcoR I  Pst I  Sal I  Kpn I \     Apa I \ BamH I    Xcm I
                            Sac I                          Acc I Asp718 I \  Bsp120 I Xma I
                            Ecl136 II                                Sac II        Sma I
```
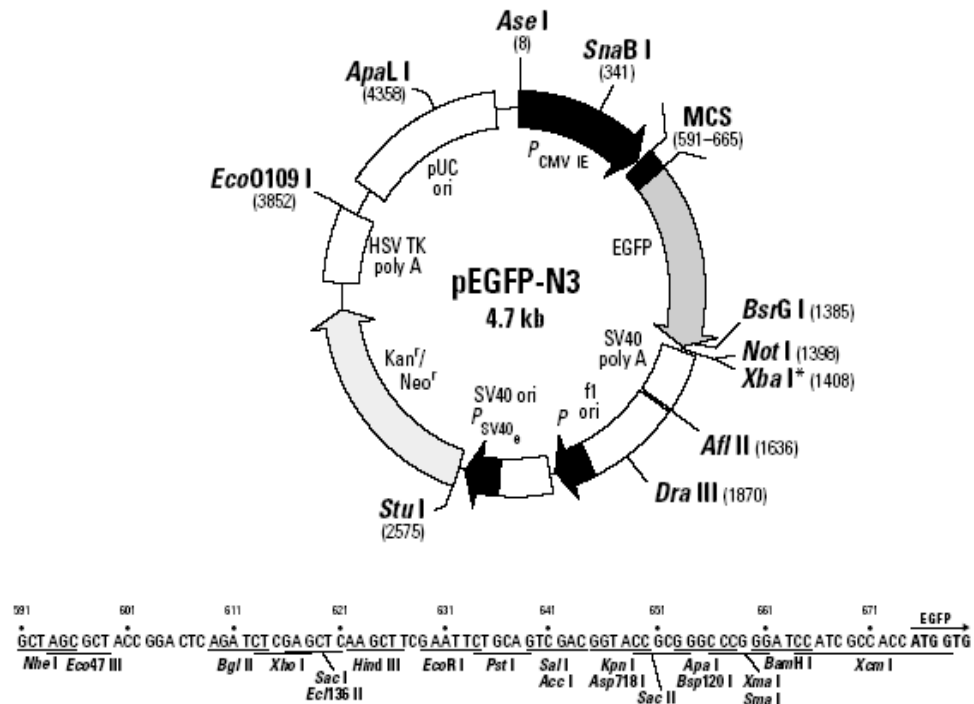
Restriction Map and Multiple Cloning Site (MCS) of pEGFP-N3 (Unique restriction sites are in bold). The Not I site follows the EGFP stop codon. The Xba I site (*) is methylated in the DNA provided by BD Biosciences Clontech. If you wish to digest the vector with this enzyme, you will need to transform the vector into a dam⁻ host and make fresh DNA.

Description:
pEGFP-N3 encodes a red-shifted variant of wild-type GFP (1–3) which has been optimized for brighter fluorescence and higher expression in mammalian cells. (Excitation maximum = 488 nm; emission maximum = 507 nm.) pEGFP-N3 encodes the GFPmut1 variant (4) which contains the double-amino-acid substitution of Phe-64 to Leu and Ser-65 to Thr. The coding sequence of the EGFP gene contains more than 190 silent base changes which correspond to human codon-usage preferences (5). Sequences flanking EGFP have been converted to a Kozak consensus translation initiation site (6) to further increase the translation efficiency in eukaryotic cells. The MCS in pEGFP-N3 is between the immediate early promoter of CMV ($P_{CMV\ IE}$) and the EGFP coding sequences. Genes cloned into the MCS will be expressed as fusions to the N terminus of EGFP if they are in the same reading frame as EGFP and there are no intervening stop codons. SV40 polyadenylation signals downstream of the EGFP gene direct proper processing of the 3' end of the EGFP mRNA. The vector backbone also contains an SV40 origin for replication in mammalian cells expressing the SV40 T-antigen. A neomycin resistance cassette (Neo^r), consisting of the SV40 early promoter, the neomycin/kanamycin resistance gene of Tn5, and polyadenylation signals from the Herpes simplex virus thymidine kinase (HSV TK) gene, allows stably transfected eukaryotic cells to be selected using G418. A bacterial promoter upstream of this cassette expresses kanamycin resistance in E. coli. The pEGFP-N3 backbone also provides a pUC origin of replication for propagation in E. coli and an f1 origin for single-stranded DNA production.

2. pCI-neo Mammalian Expression vector (Promega, E1841):
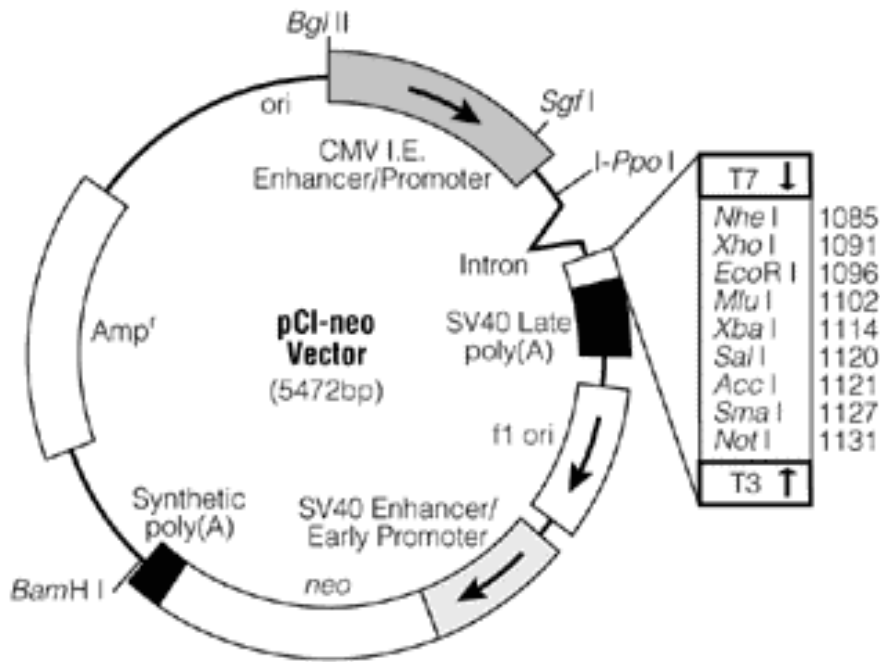
Two myc tags were engineered between the restriction sites Sal I and Not I:

Appendix C: Solutions and Kits

1. Solutions and Kits used in DNA amplification:

Kanamycin solution (Sigma, K0129), 10mg/ml.

Ampicillin solution (Aldrich, 271861), 50mg/ml.

GFX Micro Plasmid Prep Kit (Amersham Biosciences, 27-9601-01):

HiSpeed Plasmid Midi Kit (Qiagen, 12643):

Isopropanol solution (Sigma, I-9516)

100% ethanol (MERCK, K31218583), diluted by ddH$_2$O to form 70% ethanol.

EcoR I enzyme (Promega, R6011)

10X EcoR I buffer (Promega, R008A)

Not I enzyme (Promega, R6431)

10X TAE buffer (NUMI): 0.4M Tris base, Glacial Acetic acid, 0.01M EDTA

1 Kb DNA Ladder (New England BioLabs, N3232S)

6X DNA blue loading dye (Promega, G1881)

Sybr-green (Molecular Probe, S-7567)

2. Solutions used in cell culture:

DMSO (Sigma, D8418)

Penicillin-Streptomycin (Sigma, P3539)

Trypsin EDTA (Invitrogen, 25300-054)

10X PBS (NUMI): 80g/l NaCl, 2g/l KCl, 14.4g/l Na$_2$HPO$_4$, 2.4g/l KH$_2$PO$_4$, diluted to

1X PBS by Milli-Q water and autoclaved at 121˚C for 20 min before using.

7S Nerve Growth Factor (Calbiochem, 480354)

Poly-D-Lysine (Sigma, P0899)

3. Solutions and Kits used in transfection:

OPTI-MEM I Reduced Serum Medium (Invitrogen, 22600)

FuGENE 6 Transfection Reagent (Boehringer Mannheim, 85180421)

GenePORTER 2 (Gene Therapy Systems, T202007)

GeneJammer (STRATAGENE, 204130-21)

MBS Mammalian Transfection Kit (STRATAGENE, 200388)

TransIT-Neural (Mirus, NL1004)

Lipofectamine 2000 (Invitrogen, 11668-019)

TransFectin Lipid Reagent (Bio-Rad, 170-3350)

4. Solutions and Kits used for Western-blot:

RIPA buffer: 10mM Tris-HCl pH7.4, 1%NP40, 0.5% sodium deoxycholate, 150mM NaCl, 1mM EDTA, 2mM EGTA, 0.1% SDS, 25mM sodium fluoride, 2mM sodium orthovanadate, 10mM sodium pyrophosphate, Protease inhibitor tablet (Roche, 1873580)

5X SDS loading buffer: SDS 1g, 1M Tris-HCl pH6.8 3.125ml, Sucrose 5g, Bromophenol Blue 0.01g, Milli-Q water 3ml.

β-mercaptoethanol (Sigma, M6250)

RC DC protein assay kit (Bio-Rad 500-0120)

BSA (Sigma, A4503)

Resolving Gel and Stacking Gel:

Resolving Gel	Stacking Gel
Milli-Q water	Milli-Q water
30% Acrylamide/Bis	30% Acrylamide/Bis
Resolving Gel buffer	Stacking Gel buffer
10% APS	10% APS
TEMED	TEMED

5X electrophoresis buffer (NUMI): 15.1g/l Tris base, 72g/l Glycine, 5g/l SDS. Dilute

by Milli-Q water to 1X before using.

Precision Plus Protein Dual Color Standards (Bio-Rad, 161-0374)

Prestained SDS-PAGE standards, Low range (Bio-Rad, 161-0305)

10X Tris/Glycine buffer: Tris 30.3g, Glycine 144.13g, Milli-Q water top up to 1L.

Transfer buffer: 10X Tris/Glycine buffer 100ml, Milli-Q water 700ml, methanol 200ml.

5X TBS: 30.285g Tris base, 43.83g NaCl, 5M HCl adjust pH to 7.5, Milli-Q water top

up to 1L. Diluted by Milli-Q water to 1X before using.

TBST: 1L 1X TBS, 1ml Tween-20 (Baker, X251-07).

Blocking buffer: 4% skimmed milk, 1% BSA in TBST.

Stripping buffer (CHEMICON, 60513)

Primary antibodies (diluted in TBST with 5% BSA):

Anti-GFP (Roche, 181460) 1:1000

Anti-n20-p35 (Santa Cruz, Sc-821) 1:1000

Anti-c19-p35 (Santa Cruz, G302) 1:1000

Anti- α -tubuin (Sigma, T5168) 1:1000

Anti-cmyc (Santa Cruz, H201) 1:500

Anti- β -actin (Sigma, A5316) 1:1000

Secondary antibodies (diluted in blocking buffer):

Goat-anti-rabbit IgG (Bio-Rad, 170-6515) 1:10,000

Goat-anti-mouse IgG (Bio-Rad, 170-6516) 1:10:000

Chemiluminescent substrate:

West Pico (PIERCE, 34080)

West Femto (PIERCE, 34095)

5. Solutions for immunohistochemistry, DNA staining and FACS analysis:

8% paraformaldehyde (Sigma, P6148): 16g paraformaldehyde dissolve in Milli-Q water. Heat to 55 to 60˚C and add 2M NaOH until solution clears. Filter through a single use syringe filter. Dilute to 4% in PBS before using.

100mM NH_4Cl: 0.27g NH_4Cl dissolve in 50ml PBS

0.2% Triton-X 100: Triton-X 100 (Merck, 11869) dissolve in PBS

Goat Serum (Gibco, 16210-07): dilute in PBS before using

Anti-cmyc (Santa Cruz, H201) 1:250

Goat-anti-rabbit FITC conjugated 488 (Molecular Probe, 84132-1) 1:2000

Hoechst 33342 (Sigma, B2261): dilute to 5μg/ml in PBS before using

PI staining solution: 0.1% Triton-X 100, 0.2 mg/ml Rnase A (Sigma, R6513), 20μg/ml

Propidium Iodide (Sigma, P4170) in PBS.